Nonlinear Optics in Multipolar Media: Theory and Experiments

Joseph Zyss* and Isabelle Ledoux

France Telecom—Centre National d'Etudes des Télécommunications, Centre Paris B—Laboratoire de Bagneux (UA CNRS 250) Département d'Electronique Quantique et Moléculaire 196, Avenue Henri Ravera, 92225-Bagneux Cedex, France

Received July 6, 1993 (Revised Manuscript Received October 15, 1993)

Contents

I. Implication of Rotational Invariance on Nonlinear Susceptibilities: Definition of Octopolar Nonlinear Molecules

While most of the attention has traditionally been concentrated on polar nonlinear molecules and their subsequent macroscopic assemblies, a number of drawbacks have come to be identified for such structures:[1] polar molecules tend to set up more readily an antiparallel molecular arrangement, at least in the absence of more energetic intermolecular interactions such as H-bonding, and their crystallization may be disrupted by dipolar aggregation. Furthermore, the highly anisotropic structure of an optimized electrooptic crystalline material, made up of aligned polar rodlike molecules, however attractive, will limit its application to electrooptic configurations because modulating field and optical beam polarizations are both parallel to the common crystalline and molecular polar axis. More generally, when guided by the paradigm in this field of *p*-nitroaniline-like compounds and the attached two-level quantum model and electric field induced second-harmonic generation in solution, one may be wrongly induced to concentrate exclusively on one-dimensional dipolar objects, thus ignoring a wealth of possibilities from three-dimensional chemistry. This approach has been recently questioned:[1-4] it has been proposed, on the basis of experimental evidence[5,6] as well as on general tensorial and quantum mechanical considerations,[7,8] that investigations should indeed be widened so as to encompass a more diversified range of molecules with attached nonlinearities of so-called "octopolar" or more general "multipolar" origin.[1] A priori symmetry considerations may help designate molecules and materials with exact symmetry-based cancellation of their dipole moments in the excited as well as ground states and allowing for nonzero, eventually optimized quadratic microscopic β and macroscopic $\chi^{(2)}$ susceptibility tensors. It is the purpose of this work to develop this concept in terms of both its adequate tensorial framework and the molecular and material engineering pathways in the future: while the origin of the former may be traced to a number of pioneering references subsequently cited, the latter has yet to be recognized.

The approach here is more geometric and systematic than that which had lead to 3-methyl-4-nitropyridine 1-oxide (POM)[9] wherein mutual quasicancellation of submolecular dipole moments of pyridine-1 oxide and nitrobenzene moieties is ensured only for the ground state. Indeed, the maximum degree of isotropy compatible with the existence of a nonzero susceptibility tensor of rank 3 (at both molecular and macroscopic levels) will be shown to correspond to adequately defined octopolar-like systems. The intuitive relevance of these issues appears clearly when considering an atom as the ultimate example of a fully isotropic spheroidal system: owing to centrosymmetry, it cannot possess a nonzero β value. There must consequently exist a boundary separating highly anisotropic dipolar systems such as push–pull polyenes[10] from atomic-like spheroidal objects and therefore separating molecular types with nonzero β (or $\chi^{(2)}$) values from those with cancelling values.

The relevant framework to discuss these issues naturally involves the irreducible representation of rotations over tensorial sets[11] in conjunction with adequately defined multipolar groups.[1,4]

Let us briefly summarize the reasons for a tensorial framework in the present context of molecular nonlinear

0009-2665/94/0794-0077$14.00/0

Joseph Zyss was born in Neuilly, Seine, in 1950. He graduated from Ecole Polytechnique in Paris in 1972 and received a Science Doctorate (Doctorat d'Etat) in Physics from Paris VI University in 1982. He has been actively engaged in theoretical as well as experimental research in the field of molecular nonlinear optics from 1977 up to now at the Laboratoire de Bagneux (associated to CNRS) of the Centre National d'Etudes des Télécommunications, the research Laboratory of France Telecom. He is presently in charge of the Molecular Quantum Electronics Department which he set up in 1989. Dr. Zyss has authored or coauthored more than 120 research papers and 10 patents, and has edited four books in his research field. He is a member of the editorial board of *Molecular Engineering* (as associate editor) and *Nonlinear Optics*. He has held various visiting positions such as at ATT-Bell Laboratories in 1985, at MIT in 1990, and at the Weizmann Institute in 1992 as the incumbent of a Meierhof visiting professorship. He was awarded in 1987 the IBM prize in Physics of the French Physical Society. He has coordinated or participated in various collaborative research programs such as under the EEC sponsored "Esprit" framework or NRL-SDI. He is a member of various Conference Programm Committees such as the U.S. and European CLEO Conferences, the Joint ACS-OSA Symposia on Polymer Photonics and the French–Israeli Symposia on Nonlinear Optics (as co-chairman and founder). His main personal research orientations are the development of molecular engineering approaches in the field of nonlinear optics, based on a consistent set of experiments and models that has lead to the conception of "optimized" molecular and crystalline structures, the investigation of efficient three-wave-mixing processes ranging from second-harmonic generation to near-infrared optical parametric oscillation in a variety of molecular media such as thin films, molecular crystals, or Langmuir–Blodgett layers, and, more recently, the conception and demonstration of active and passive polymer-based optoelectronic devices for telecommunications related applications.

Isabelle Ledoux was born in Rome, Italy, in 1957. She graduated from the Ecole Normale Supérieure, Paris, France, in 1981, and received an engineering degree from the Ecole Nationale Supérieure des Télécommunications, Paris, in 1983. After one year spent at Thomson-CSF Research laboratory, she joined the Centre National d'Etudes des Télécommunications (CNET), Bagneux, France, in 1983. She received her Ph.D. in 1988, on "Parametric effects in highly nonlinear organic compounds: solutions, single crystals, thin films". She was awarded the 1989 prize for Chemical Physics from the French Chemical Society. In the Department "Electronique Quantique et Moléculaire", she is now leading the research group in molecular engineering and nonlinear spectroscopy. Her current domains of interest are nonlinear spectroscopy of polyenes and molecular engineering of organometallic compounds. She is author or coauthor of 70 original papers.

optics. Tensors are of widespread use in various domains of physics (optics, mechanics, and acoustics, for example) whenever the anisotropy of a system, and hence of its response to some external solicitation, plays an important part. For example, in the realm of optics, whereas the optical dielectric properties of an isotropic medium can be accounted for by a single scalar ϵ connecting the **D** and **E** fields, a symmetric 3×3 ϵ_{ij} matrix is needed in the case of anisotropic media such as biaxial crystals and most uniaxial ones as well as poled polymers or liquid crystals (not to mention additional gyrotropic and magnetic effects). In the simpler case of isotropic systems such as atoms, the scalar description is valid at all order of expansion of the response in terms of the input parameter, with nonlinear scalar constants accounting for higher order nonlinear phenomena. In the present context of nonlinear optical phenomena in molecular media, the pertubating input is the optical field **E** which polarizes the electronic charge, thus leading to an induced dipole moment **P**. A multilinear expansion of **P** in terms of **E**, inasmuch as the perturbation regime is valid, accounts for this phenomenon according to

$$P_i = P_i + \alpha_{ij}E_j + \beta_{ijk}E_jE_k + \gamma_{ijkl}E_jE_kE_l + \ldots \quad (1)$$

Following the so-called Einstein convention, repeated indices are summed with i, j, and k spanning the three directions of space. It is convenient to choose a Cartesian framework with axis x, y, and z adapted to the symmetry of the molecule which helps reveal a reduction of the number of independent coefficients in the expansion. The ability of this formalism to account for anisotropic linear as well as nonlinear polarization mechanisms stems from the distinction between different α, β, and γ susceptibility terms: these are made by adequate indexation over the directions of space, to depend on the input field polarizations. Rigorous justification of the validity of this expansion can be shown to result from causality and time invariance properties of the polarization response.[12] One may want to consider (hyper)polarizability coefficients as partial derivatives of increasing order of **P** components with respect to **E** components, namely

$$\alpha_{ij} = \frac{\partial P_i}{\partial E_j} \text{ or } [\alpha] = \vec{\nabla}_{\vec{E}}\vec{P} \quad (2)$$

$$\beta_{ijk} = 1/2\,\frac{\partial^2 P_i}{\partial E_j \partial E_k} \text{ or } [\beta] = 1/2\,\vec{\nabla}_{\vec{E}}\vec{\nabla}_{\vec{E}}\vec{P} \quad (3)$$

$$\gamma_{ijk} = 1/3!\,\frac{\partial^3 P_i}{\partial E_j \partial E_k \partial E_l} \text{ or } [\gamma] = 1/3!\,\vec{\nabla}_{\vec{E}}\vec{\nabla}_{\vec{E}}\vec{\nabla}_{\vec{E}}\vec{P} \quad (4)$$

where $\vec{\nabla}_{\vec{E}}$ represents the gradient operator with respect to $\vec{E}$.

In the general case of a rank-n tensor $T^{(n)}$ (the rank being the number of Cartesian indices needed to label the coefficients of a tensor, e.g. a matrix is a rank-2 tensor), the general expression accounting for the

rotation from the orthogonal reference frame $\{x,y,z\}$ onto a new frame $\{x',y',z'\}$ is

$$T^{(n)}_{i'_1 i'_2 \ldots i'_n} = R_{i'_1 i_1} R_{i'_2 i_2} \ldots R_{i'_n i_n} T_{i_1 i_2 \ldots i_n} \quad (5)$$

where R is the rotation matrix connecting the two frames with $R_{i'j i_j} = \cos(\vec{i'}_j, \vec{i}_j)$. Rotation of susceptibility tensors is required to describe optical phenomena in materials where molecules are angularly distributed in regular (e.g. single crystals) or statistical (e.g. polymers or mesophases) arrangements. In the framework of the oriented gas model, summation over a statistically weighed ensemble of molecules with a distribution of orientations is performed after rotation from the microscopic molecular framework onto a single common macroscopic framework conventionally attached to the crystalline symmetry axis or to the poling and substrate directions in the case of poled polymer films. In this context, a major drawback of the Cartesian representation used in expressions 1 and 5 is the scrambling of all components resulting in a loss of molecular intuition after averaging at the macroscopic scale.

In contrast with the Cartesian formalism, the so-called irreducible representation of tensorial properties permits one to handle rotation of tensorial properties in a simpler way by grouping of Cartesian components in adequately defined linear combinations with "universal" tabulated coefficients. In Appendix A, we propose a brief introduction to the irreducible tensor formalism, which does not require going through algebraic technicalities of group representation theory but starts from the more familiar 2-D and 3-D Fourier functional expansions. In particular, eq A14 provides a means to derive irreducible tensorial components from Cartesian components. We have assumed in this appendix, as well as in the following, nonresonant processes resulting in the validity of Kleinman symmetry conditions and hence susceptibility tensors invariant with respect to permutation of their Cartesian indices. As a general result of irreducible tensor representation theory, one may decompose any tensor $T^{(n)}$ of arbitrary rank n in a sum of so-called irreducible components $T_j^{(n),\tau_J}$, following

$$T^{(n)} = \sum_{J=0,\tau_J}^{n} T_J^{(n),\tau_J} \quad (6)$$

The so-called seniority index τ_J is eventually introduced to help distinguish between different components of identical weight J. Each irreducible tensorial set is spanned by $2J + 1$ independent components labeled by the integer m running from $-J$ to J, hence the following more complete decomposition:

$$T^{(n)} = \sum_{J=0}^{n} \sum_{m=-J}^{J} \sum_{\tau_J} T^{(n),\tau_J}_{J,m} \quad (7)$$

Most noteworthy is the fact that the summation over weights J extends up to rank n only and will only involve, owing to index permutation symmetry, odd integers for $n = 2p + 1$ (odd-rank tensor or even-order susceptibility such as β or $\chi^{(2)}$ according to current conventions) and even-order integers for $n = 2p$ (even-rank tensors or odd-order susceptibilities such as $\chi^{(1)}$ or $\chi^{(3)}$). This truncated summation obviously contrasts with similar ones in the realm of infinite functional spaces where, for example, a regular angular function defined on the unit sphere may be classically expanded over an infinity of (J,m) indexed Y^J_m spherical harmonics, whereas the finite dimension of tensorial spaces of present interest limits the summation. Furthermore, the $\mathbf{T}^{(n),\tau_J}_{J,m}$'s satisfy a closure condition with respect to the application of rotations, namely

$$R(\theta,\phi,\psi)[\mathbf{T}^{(n),\tau_J}_{J,m}] = \sum_{m'=-J}^{J} D^J_{m,m'}(\theta,\phi,\psi)\mathbf{T}^{(n),\tau_J}_{J,m'} \quad (8)$$

The $D^j_{m,m'}$ are the Wigner matrix elements depending on the three Euler angles which define the rotation.[11] This decomposition had been initially developed and widely documented in the framework of atomic angular momentum composition, while its transposition to the tensorial description of nonlinear optical (NLO) phenomena has been worked out.[13-15] However, molecular and material engineering insights and implications, as detailed hereafter, may not have been recognized at the time, such as the identification of electronic and structural parameters underlying the irreducible components of nonlinear susceptibilities and subsequent molecular engineering possibilities.

It turns out from the truncation on J in eq 7 that β (or $\chi^{(2)}$) will only have two components of order 1 and 3, respectively referred to as the dipolar and octopolar irreducible components:

$$\beta = \beta_{J=1} \oplus \beta_{J=3} \quad (9)$$

This expression, and its generalization to higher order susceptibilities (e.g. $\gamma = \gamma_{J=0} + \gamma_{J=2} + \gamma_{J=4}$, etc.) can be viewed as a rotational Fourier expansion with the irreducible J components spanning the rotational spectrum of the molecule or material. As is well known in Fourier theory, the successive terms of a Fourier series must not decrease to ensure convergence, hence the formal possibility, at this stage, of optimizing higher J components. In the case of the β tensor, its vectorial component ($J = 1$) allows for three independent coefficients ($-1 \le m \le 1$), while the octopolar component may accommodate seven components ($-3 \le m \le 3$), thus making up for the 10 components of a symmetric rank-3 tensor.

It is worthwhile to generalize the constraint of dipole cancellation into that of multipole cancellation. This is readily done by referring to the following adequate definition of multipolar groups: a multipolar group of order J may be defined as a point group, whether it is linked to molecular or crystalline systems, where all tensorial properties of order strictly lower than J are strictly canceling. That this definition is valid and intrinsic is justified by adequate manipulation of character tables and application of Schur's lemma as detailed in Appendix B. According to that definition, a molecule or a material belongs to an octopolar group ($J = 3$) when all dipolar-like quantities (e.g. dipole moment, vector part of β, etc.) vanish, while there still remains a nonzero β tensor reduced to the symmetry-allowed octopolar component contribution (see eq 9).

Octopolar groups, such as the D_{3h} group, the tetrahedral cubic group T_d, or quadrupolar groups ($J = 2$) such as the orthorhombic 222 group (e.g. POM crystalline structure) will lead to more isotropic objects than those belonging to lower order eventually polar groups,

but are still compatible with β or $\chi^{(2)}$ properties. Such would not be the case for hexadecapolar groups (J = 4) as well as other multipolar groups of order J strictly larger than 3.

However, a slight restriction obviously comes in in the case of odd-order susceptibilities which always contain a nonzero scalar (J = 0) component corresponding to the so-called isotropic or fully symmetrical component. The D_{4h} hexadecapolar group of phthalocyanines can for example be viewed as the highest n-fold symmetry group compatible with the existence of a nonzero nonisotropic (i.e. $J \neq 0$) γ cubic hyperpolarizability contribution (namely $\chi^{(3)}_{J=4}$). Above n = 4, $\chi^{(3)}$ will reduce to its sole isotropic scalar component and will "average" out the anisotropy of the molecules. Hypothetical higher order nonlinear effects and related susceptibilities would however increasingly reflect molecular anisotropy.

Finally, an interesting nonintuitive consequence of these considerations can be derived as to the issue of a nonzero, however possibly small, β tensor, for any noncentrosymmetric molecule: according to the previous definitions, when a noncentrosymmetric molecule belongs to a multipolar group of order strictly higher than 3 (i.e. 5 or more, 4 being irrelevant in the context of β tensors) then, owing to the absence of irreducible components of order higher than 3 in the rotational spectrum of the β tensor, the conclusion is that β must strictly vanish. For example, a 5-fold symmetry molecule, such as a hypothetically eclipsed ferrocene ion, cannot sustain a nonzero β tensor although it is noncentrosymmetric. These considerations underlie our present emphasis on octopolar (J = 3 multipolar) systems, as opposed to higher order 2^J multipoles, in the context of quadratic nonlinear optics.

These considerations are summarized in the case of planar molecules in Figure 1. Any arbitrary charge distribution $F(\mathbf{r},\theta)$ may be expanded in a sum of simpler more symmetrical rotational harmonics with increasing J-fold rotational symmetry invariance. This is a straightforward result of Fourier theory as recalled in Appendix A. The symmetry group of each individual component is then multipolar of order J according to the previously given definition (see Appendix B). The weight of nonzero irreducible components of optical susceptibilities attached to a given component of J multipolar symmetry cannot be smaller than J (except for J = 0). As J increases, remembering that the highest order in the irreducible spectrum of a tensor is limited by its rank, the symmetry conditions will fully cancel any susceptibility of rank lower than J (i.e. of order strictly lower than $J-1$). As discussed in Appendix B, scalar (J = 0) components of even-rank (odd-order) susceptibilities are an exception and cannot be made to cancel: therefore odd-order susceptibilities (e.g. $\chi^{(3)}$) will not fully vanish but will be rotationally averaged and made to be restricted to their scalar component, as opposed to even-order susceptibilities which may be fully canceled by symmetry.

In the context of nonlinear optics, we refer in a self-understood way to "octopolar nonlinear molecules" by way of abbreviation for the more explicit, however tedious, full reference to molecules with a β tensor reduced to a single J = 3 component of octopolar

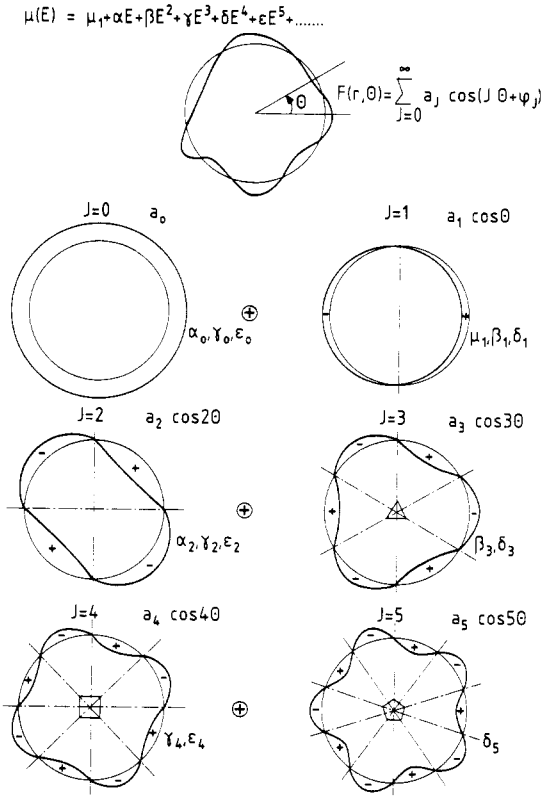

Figure 1. Angular Fourier decomposition of an arbitrary charge distribution in more symmetric components of multipolar nature (rotational frequencies). μ_J, α_J, β_J, γ_J, δ_J, and ϵ_J refer to irreducible components of weight J of the dipole (with J = 1 as the sole possibility for μ_J), polarizability and hyperpolarizability tensors up to fifth-order processes, J being no larger than the corresponding tensorial rank. For all rotational harmonics, scalar (J = 0) components are still present but omitted in the figure (except for the J = 0 harmonic itself) for simplicity.

symmetry. In fact, octopolar nonlinear molecules may well sustain a nonzero, however generally small, quadrupolar tension in the usual meaning: the fully symmetrical J = 0 component of an even-rank tensor, such as that of the rank-2 quadrupolar tensor, does not vanish under multipolar symmetry constraints of higher order, as already mentioned for odd-order, even-rank susceptibilities. Nevertheless, in cases discussed hereafter, such as planar D_{3h} systems,[5] the "classical" molecular quadrupolar tensor turns out to be small, if not negligible, as suggested by approximating the molecule by an equivalent point-charge distribution located at atomic sites, an approximation which then entails strict cancellation of the quadrupole. Various octopolar point-charge distributions are represented in Figure 2 from which actual molecules possibly meeting the additional requirements for quadratic nonlinear efficiency (conjugation, intramolecular charge transfer etc.) are to be derived as will be subsequently exemplified.

The adequate tensorial framework, in particular with respect to the respective rotational behaviours of the J = 1 and J = 3 irreducible components is detailed in section II. On the basis of this decomposition scheme, a vectorial representation is subsequently introduced in section III and shown to permit classification of nonlinear molecules and materials in a general and intrinsic way encompassing the two extreme cases of purely J = 1 and J = 3 nonlinearities as boundary

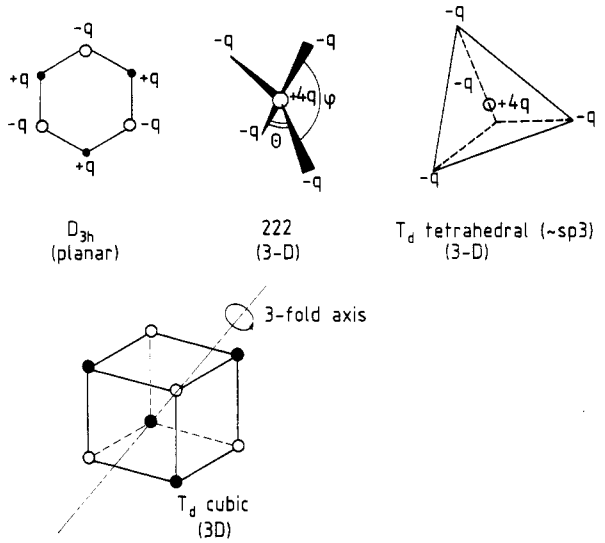

Figure 2. Various 2-D and 3-D simple octopolar point charge distributions. The cubic T_d distribution made up of alternated charges at the edges of a cube stands for a simple 3-D octopole. It projects, along one of its three equivalent 3-fold symmetry axes (cube diagonals), onto a planar 2-D octopole with D_{3h} symmetry.

situations. Molecular engineering directions for both planar and nonplanar systems are then proposed. Quantum mechanical implications are discussed in section IV, and the relevance of three-level systems instead of the presently inadequate two-level model is pointed out. In section V, experimental determination of typical octopolar molecules such as crystal violet and ruthenium complexes is reported, taking into account symmetry considerations and tensorial averaging in solution. Macroscopic structural and optical considerations are outlined in section VI: the problem of ordering octopolar molecules into adequately defined octopolar assemblies is discussed and the associated macroscopic octopolar order parameters defined in simple cases. Symmetry considerations, applied consistently to the interacting optical beam electric fields and to the nonlinear susceptibility, designate circularly polarized beams as symmetry-adapted optical probes of irreducible susceptibility components.

II. Tensorial Properties of Octopolar Nonlinear Molecules

The general tensorial framework to manipulate octopolar systems is presented in this section with details deferred to the accompanying appendices: the behavior of octopolar ($J = 3$) planar symmetric tensors under rotation will be seen to generalize in a recursive manner over that of lower order tensors, namely $J = 1$ (vector) and $J = 2$ (quadrupole as a traceless symmetric tensor). We will constantly refer in the following to a prototypical couple of corresponding dipolar and octopolar planar trigonal systems [e.g. *p*-nitroaniline (pNA) and trinitrotriaminobenzene (TATB)] with axis defined as in Figure 3. Planar molecules, such as conjugated aromatic systems or some triphenylmethane (TPM) dyes, are of great practical and conceptual importance and will be the first to be discussed. Octopolar molecules can however adopt out-of-plane structures of great interest, including chiral geometries:[6] the more general case of 3-D systems is

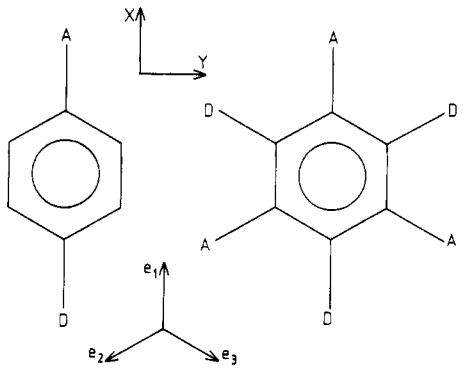

Figure 3. Corresponding polar and trigonal octopolar systems with conventions for reference axis.

therefore dealt with in Appendices C and D with related molecular engineering propositions defered to section III.

We concentrate hereafter on the dipole μ, the polarizability α and first-order hyperpolarizability β: α is assumed to be a purely quadrupolar ($J = 2$) traceless rank 2 tensor and β a purely octopolar ($J = 3$) tensor. All three tensors above happen to belong to tensorial spaces of same dimension where, for convenience, the following respective basis sets and corresponding decompositions have been worked out:

$$\mu = \mu_X \mathbf{e}_X + \mu_Y \mathbf{e}_Y \tag{10}$$

$$\alpha = \alpha_1 \mathbf{Q}_{XX} + \alpha_2 \mathbf{Q}_{XY} \tag{11}$$

$$\beta = \beta_1 \mathbf{O}_X + \beta_2 \mathbf{O}_Y \tag{12}$$

with

$$\mathbf{Q}_{XX} = \mathbf{e}_X \otimes \mathbf{e}_X - \mathbf{e}_Y \otimes \mathbf{e}_Y \tag{13}$$

$$\mathbf{Q}_{XY} = 2\mathbf{e}_X \otimes \mathbf{e}_Y \tag{14}$$

$$\mathbf{O}_X = \mathbf{e}_X \otimes \mathbf{e}_X \otimes \mathbf{e}_X - 3\mathbf{e}_X \otimes \mathbf{e}_Y \otimes \mathbf{e}_Y \tag{15}$$

$$\mathbf{O}_Y = 3\mathbf{e}_Y \otimes \mathbf{e}_X \otimes \mathbf{e}_X - \mathbf{e}_Y \otimes \mathbf{e}_Y \otimes \mathbf{e}_Y \tag{16}$$

The rotational behavior of the dipole and (hyper)-polarizability tensors may then be straightforwardly established:

$$\mathbf{e}_X' = \cos\psi\, \mathbf{e}_X + \sin\psi\, \mathbf{e}_Y \tag{17}$$

$$\mathbf{e}_Y' = \cos\psi\, \mathbf{e}_Y - \sin\psi\, \mathbf{e}_X \tag{18}$$

$$\mathbf{Q}_{XX}' = \cos 2\psi\, \mathbf{Q}_{XX} + \sin 2\psi\, \mathbf{Q}_{XY} \tag{19}$$

$$\mathbf{Q}_{YY}' = \cos 2\psi\, \mathbf{Q}_{XY} - \sin 2\psi\, \mathbf{Q}_{XX} \tag{20}$$

$$\mathbf{O}_X' = \cos 3\psi\, \mathbf{O}_X + \sin 3\psi\, \mathbf{O}_Y \tag{21}$$

$$\mathbf{O}_Y' = \cos 3\psi\, \mathbf{O}_Y - \sin 3\psi\, \mathbf{O}_X \tag{22}$$

where the primed letters refer to rotated tensors by an angle ψ along an axis perpendicular to the molecular plane. This allows one to obtain simple transformation rules for the α and β components under rotation which simply generalize over the usual vectorial rotation laws by replacement of ψ by 2ψ and 3ψ in the respective

cases of quadrupoles and octopoles. In the case of a "pure" octopole of D_{3h} planar symmetry with the following expression:

$$\beta = \beta_{XXX} \boldsymbol{O}_X \tag{23}$$

a rotation will readily transform β into β' given by

$$\beta' = R[\beta] = \beta_{XXX}(\cos 3\psi\ \boldsymbol{O}_X + \sin 3\psi\ \boldsymbol{O}_Y) \tag{24}$$

A different approach, based more on chemical intuition than on abstract geometrical considerations, leads to the same expression as in eqs 21 and 22, however with some additional assumption as to the polarization mechanism driving the nonlinearity. A planar trigonal molecule, such as exemplified by TATB[5,16] can be decomposed into a sum of three interacting subsystems respectively oriented along $\boldsymbol{e}_1$, $\boldsymbol{e}_2$, and $\boldsymbol{e}_3$ (see Figure 3 for conventions). The low-lying electronic states of these subsystems may be ascribed, in a grossly simplified manner for the sake of clarity, to a "para" intramolecular charge-transfer state leading to β_{para}, opposed to two parallel equivalent "ortho" states underlying β_{ortho}. Assuming additivity, i.e. weak interaction of these subexcitations, in fact an oversimplifying assumption to be questioned in section IV, leads to

$$\beta = m(\boldsymbol{e}_1 \otimes \boldsymbol{e}_1 \otimes \boldsymbol{e}_1 + \boldsymbol{e}_2 \otimes \boldsymbol{e}_2 \otimes \boldsymbol{e}_2 + \boldsymbol{e}_3 \otimes \boldsymbol{e}_3 \otimes \boldsymbol{e}_3) \tag{25}$$

with $m = \beta = \beta_{para} - 2\beta_{ortho}$.

Applying, as from trigonal symmetry, $\boldsymbol{e}_1 + \boldsymbol{e}_2 + \boldsymbol{e}_3 = \boldsymbol{O}$ and introducing the orthonormal basis set $(\boldsymbol{e}_x, \boldsymbol{e}_y)$, the multilinearity of the tensorial product[17] leads straightforwardly to

$$\beta = 3m/4(\boldsymbol{e}_X \otimes \boldsymbol{e}_X \otimes \boldsymbol{e}_X - \boldsymbol{e}_X \otimes \boldsymbol{e}_Y \otimes \boldsymbol{e}_Y - \boldsymbol{e}_Y \otimes \boldsymbol{e}_X \otimes \boldsymbol{e}_Y - \boldsymbol{e}_Y \otimes \boldsymbol{e}_Y \otimes \boldsymbol{e}_X) \tag{26}$$

Condensation of the last three symmetry-equivalent tensorial basis tensors in eq 26 leads to the same result as in eqs 15 and 23. The underlying assumption, to be further questioned in the next sections, has to do with the additivity and hence negligible interactions between the "elementary" para and ortho charge-transfer interactions. While the symmetry part in eqs 23 and 26 is identical and does not depend on the additivity assumption, the magnitude of β suggested by eq 26 is a direct consequence of the additivity hypothesis.

The next crucial issue is the estimation of the relative magnitude of the nonlinearities of corresponding polar disubstituted and octopolar hexasubstituted systems such as, for example, *p*-nitroaniline and TATB. The squared norm of a Cartesian tensor defined with respect to an orthonormal vectorial basis set is given by the sum of its squared Cartesian coefficients, with care being paid to symmetry reduction:

$$\|\beta\|^2 = \sum_{i,j,k} {\beta_{ijk}}^2 \tag{27}$$

A proper definition of the norm of the irreducible components of a tensor should ensure compliance with both a generalized Pythagorein theorem as well as the linear "closure" or projection condition leading to

$$\|\beta\|^2 = \|\beta_{J=1}\|^2 + \|\beta_{J=3}\|^2 \tag{28}$$

$$\beta = \beta_{J=1} + \beta_{J=3} \tag{29}$$

The following expressions may then be shown to uniquely comply with these conditions in the case of a 2-D planar system with no further symmetry assumptions, as had been initially proposed to describe the properties of methyl [(2,4-dinitrophenyl)amino]propanoate (MAP):[18]

$$\beta = \beta_{XXX}\boldsymbol{e}_X \otimes \boldsymbol{e}_X \otimes \boldsymbol{e}_X + \beta_{YYY}\boldsymbol{e}_Y \otimes \boldsymbol{e}_Y \otimes \boldsymbol{e}_Y + 3\beta_{XYY}\boldsymbol{e}_X \otimes \boldsymbol{e}_Y \otimes \boldsymbol{e}_Y + 3\beta_{YXX}\boldsymbol{e}_Y \otimes \boldsymbol{e}_X \otimes \boldsymbol{e}_x \tag{30}$$

$$\beta_{J=1} = 3/4\ [(\beta_{XXX} + \beta_{XYY})\boldsymbol{e}_X + (\beta_{YYY} + \beta_{YXX})\boldsymbol{e}_Y] \otimes (\boldsymbol{e}_X \otimes \boldsymbol{e}_X + \boldsymbol{e}_Y \otimes \boldsymbol{e}_Y) \tag{31}$$

$$\beta_{J=3} = 1/4\ (\beta_{XXX} - 3\beta_{XYY})\boldsymbol{e}_X \otimes (\boldsymbol{e}_X \otimes \boldsymbol{e}_X - 3\boldsymbol{e}_Y \otimes \boldsymbol{e}_Y) + 1/4\ (\beta_{YXX})\boldsymbol{e}_Y \otimes (e_Y \otimes \boldsymbol{e}_Y - 3\boldsymbol{e}_X \otimes \boldsymbol{e}_X) \tag{32}$$

$$\|\beta\|^2 = {\beta_{XXX}}^2 + {\beta_{YYY}}^2 + 3{\beta_{XYY}}^2 + 3{\beta_{YXX}}^2 \tag{33}$$

$$\|\beta_{J=1}\|^2 = 3/4\ [(\beta_{XYY} + \beta_{XYY})^2 + (\beta_{YYY} + \beta_{1YXX})^2] \tag{34}$$

$$\|\beta_{J=3}\|^2 = 1/4\ [(\beta_{XXX} - 3\beta_{XYY})^2 + (\beta_{YYY} - 3\beta_{YXX})^2] \tag{35}$$

In the special case of a planar system with *mm*2 symmetry, such as the *p*-nitroaniline molecule, the additional condition $\beta_{YYY} = \beta_{YXX} = 0$ (where X is the 2-fold symmetry axis) has to be introduced in these expressions. Furthermore, in the case of a planar system with D_{3h} symmetry, such as TATB, $\beta_{XYY} = -\beta_{XXX}$, which cancels the vectorial component and leads to

$$\|\beta_{J=3}\| = 2\beta_{XXX} = \|\beta\| \tag{36}$$

For a 1-D system[19] whereby $\beta = \beta_{XXX}\boldsymbol{e}_X \otimes \boldsymbol{e}_X \otimes \boldsymbol{e}_X$, the following normalization is obtained:

$$\|\beta_{J=1}\| = \sqrt{3}/2\ \beta_{XXX} \tag{37}$$

$$\|\beta_{J=3}\| = 1/2\ \beta_{XXX} \tag{38}$$

Assuming the same β_{XXX} coefficient, this gives an obvious advantage to octopolar molecules over corresponding 1-D systems (e.g. the pNA–TATB couple), by simply opening up the dipolar molecule into a less anisotropic system: that this can indeed be done at no significant cost to β_{XXX} is justified elsewhere (see section IV and references therein). A more systematic account of irreducible β-tensor decomposition for the main point groups and both 2-D and 3-D molecules is to be found in Appendix C. Furthermore, we generalize in Appendix D the previous considerations to the situation where the 2-D system is embedded in 3-D space so as to account for possibly significant out-of-plane interactions, whereas previous considerations relate to fully confined 2-D systems (i.e. molecule as well as interactions constrained to a plane).

The parameter ρ, defined hereafter in the case of a C_{2v} molecule, is convenient to compare the relative magnitudes of the octopolar and dipolar components of a molecular quadratic hyperpolarizability:[3]

$$\rho = \frac{\|\beta_{J=3}\|}{\|\beta_{J=1}\|} = 1/\sqrt{3}\left|\frac{\beta_{XXX} - 3\beta_{XYY}}{\beta_{XXX} + \beta_{XYY}}\right| = 1/\sqrt{3}\left|\frac{1 - 3u}{1 + u}\right| \tag{39}$$

where the variable $u = \beta_{XYY}/\beta_{XXX}$ reflects the anisotropy

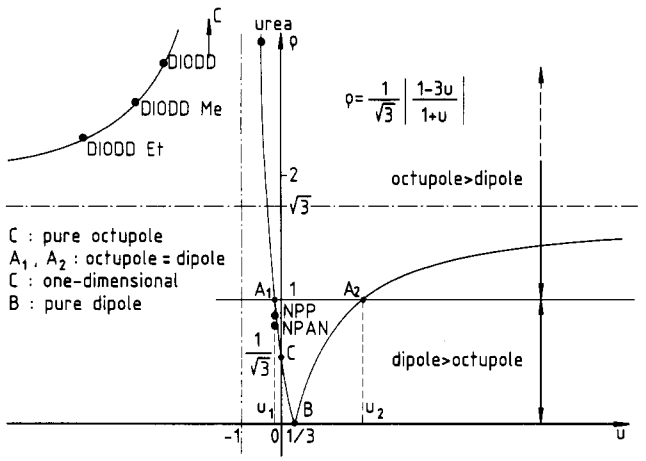

Figure 4. Dependence of ρ (ratio of octopolar over dipolar contributions) on parameter $u = \beta_{XYY}/\beta_{XXX}$ measuring the in-plane anisotropy of the β tensor in the case of a C_{2v} molecule. The (ρ,u) values are given for selected molecules detailed hereafter: NPP;[21] NPAN[22,23] (data for NPP and NPAN are both from ref 23); urea;[24] 3-amino-4,6-dinitroaniline (DIODD);[20] DIODD Me and DIODD Et are analog to DIODD except for methyl and ethyl groups, instead of hydrogen on the amino groups.

of the in-plane nonlinearity. Generalization of this expression of the 3-D case can be found in Appendix D. Considerations pertaining to the balance between "diagonal" and "off-diagonal" β-tensor coefficients are to be found in a specific case in ref 20. Expression 39 provides an adequate quantitative way toward the classification of molecular systems in terms of their more or less pronounced octopolar versus dipolar character. Variations of ρ with respect to u are displayed in Figure 4. The (ρ,u) quadrangle can be divided in two halves, respectively above and below the $\rho = 1$ axis. The upper (and, respectively lower) zone, for $u > u_2$ and $u < u_1$ ($u_1 < u < u_2$), corresponds to a molecule of more pronounced octopolar (dipolar) character. The value of u_1 (u_2) is $(1-\sqrt{3})/\sqrt{3}(1+\sqrt{3})$ $((\sqrt{3}+1)/\sqrt{3}(\sqrt{3}-1))$. The octopolar (dipolar) contribution peaks for $u = -1$ ($u = {}^1/_3$) corresponding to no dipole (octopole) and hence a pure octopolar (dipolar) system. For $u = 0$, the molecular hyperpolarizability corresponds to the well-documented "one-dimensional" system[19] whereby β reduces to a single β_{XXX} component and $\rho = 1/\sqrt{3}$. In this case the system allows for both octopolar and dipolar components, the latter being predominant. The ratio ρ will depend on structural features underlying the molecular polarization anisotropy with various examples displayed in Table 1 and further discussed in the next section. The parameter ρ is exemplified in Table 1 for a selection of representative molecules spanning the (ρ,u) plane. TATB and other octopolar chromophores are not represented within Figure 4 as they correspond to the infinitely distant asymptotic "0C" position (infinite ρ for $u = -1$). The most octopolar-like species are urea and the N,N′-dioctadecyl-4,6-dinitro-1,3-diaminobenzene (DIODD) analogs:[20] the latter are particularly remarkable in view of their higher off-diagonal β_{XYY} coefficients surpassing the β_{XXX} coefficient by a factor of 3–4. *N*-(4-Nitrophenyl)-L-prolinol (NPP)[21] and *N*-(4-nitrophenyl)-*N*-methylacetonitrile (NPAN)[22,23] exhibit relatively balanced octopolar and dipolar contributions. MAP[25] is not represented as it does not satisfy *mm*2 symmetry. In this case, eq 39 must be generalized as follows

$$3\rho^2 = \frac{(1-3u_X)^2 + \nu(1-3u_Y)^2}{(1+u_X)^2 + (1+u_Y)^2} \qquad (40)$$

with $u_X = \beta_{XYY}/\beta_{XXX}$, $u_Y = \beta_{YXX}/\beta_{YYY}$, and $\nu = \beta_{YYY}/\beta_{XXX}$.

Table 1. Various Nonlinear Molecules with Corresponding β Tensor Coefficients (in 10^{30} esu Units), μ, and ρ (Dimensionless Values)[a]

molecules	β_{xyz}	β_{xxx}	$u = \beta_{xyz}/\beta_{xxx}$	ρ
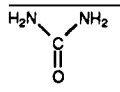 urea	0.60	−1.14	−0.52	3.09
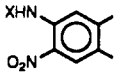 X = H	9.87	−3.11	−3.17	2.80
X = CH_3	12.1	−3.10	−3.94	2.52
X = C_2H_5	13.6	−2.80	−4.89	2.32
"DIODD" analogs				
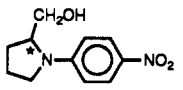 NPP	2.3	−17.2	−0.134	0.93
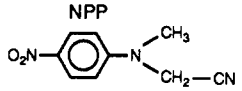 NPAN	2.3	−11.9	−0.193	0.912
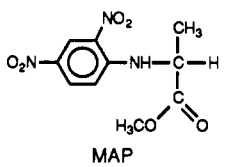 MAP	−0.48	−27		0.744

[a] The origin of data is detailed in the caption of Figure 4 except for MAP (ref 18). Urea and DIODD analogs display accurate *mm*2 symmetry; NPP and NPAN are approximated by quasi-*mm*2 structures as far as their polarizabilities are concerned; MAP is dealt with as a quasiplanar molecule with no further symmetry. The X direction is along the quasi-2-fold axis for *mm*2-like structures and along the *p*-nitro to amino-like groups for MAP.

III. A General Vectorial Classification Scheme for Nonlinear Molecules: Toward the Engineering of Octopolar Nonlinear Molecules

Traditional comparison and classification schemes of quadratic nonlinear molecules have been biased by the prevailing two-level quantum model of β and the electric-field-induced second-harmonic (EFISH) experimental technique which, by nature, leaves aside contributions to β other than the dipolar one, furthermore projected on the direction of the ground-state dipole moment. This situation reflects on the classification of molecules in terms of their nonlinear susceptibilities, which, following EFISH data, will then scale with the projection of the dipolar component of β on the ground-state dipole moment. This may lead to a partial, at best, and possibly erratic classification due to the double ignorance of both the $J = 3$ octopolar contribution to β (possibly the sole one for octopolar molecules as depicted here) and of the angle between $\beta_{J=1}$ and the dipole moment.

A more adequate scheme based on the previous considerations, and which may encompass prior con-

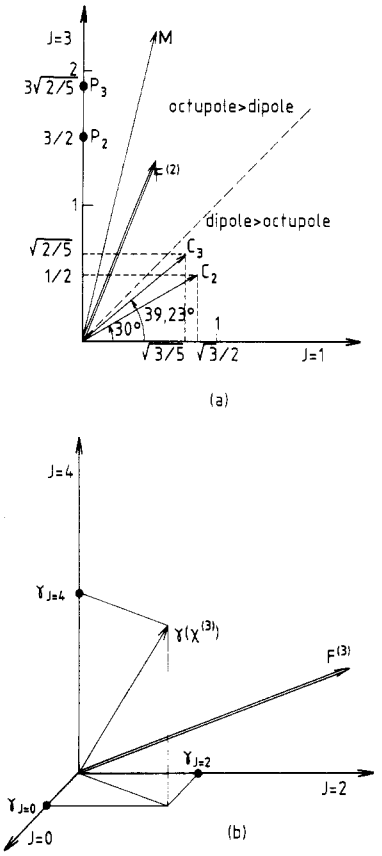

Figure 5. Reference vectorial representation scheme for quadratic nonlinear susceptibilities of anisotropic molecules and materials. In part a, the representation plane is spanned by the irreducible tensorial components $J = 1$ and $J = 3$. M stands for the quadratic susceptibility of a given molecule or material and $F^{(2)}$ for the corresponding field tensor. $C_{2,3}$ stands for a purely 1-D β tensor with $P_{2,3}$ deduced by simple tensorial addition. Utilization of a 2-D or 3-D formalism is reflected by the subscript 2 or 3.
In Part b, a similar 3-D vectorial decomposition scheme is applied to third-order susceptibilities $F^{(3)}$ stands for the cubic, rank-4 field tensor.

ceptions as boundary cases, is proposed hereafter and shown to take fully into account all anisotropic multipolar contributions. Its main features are summarized and illustrated in Figure 5. In this vectorial planar representation, the β or $\chi^{(2)}$ tensorial space is decomposed into $J = 1$ (dipolar) and $J = 3$ (octopolar) orthogonal subspaces, the projections of β onto these subspaces standing respectively for $\beta_{J=1}$ and $\beta_{J=3}$ as shown in Figure 5a. A similar vectorial scheme leads to a representation of the rank-3 γ hyperpolarizability or $\chi^{(3)}$ susceptibility tensors in a 3-D vector space spanned by the $J = 0$, 2, and 4 irreducible representations of symmetric rank-4 tensors as in Figure 5b (assuming there again Kleinman conditions fulfilled).

In the case of quadratic (or cubic) processes, the corresponding rank-3 (rank-4) field tensor[1,26] may be defined as

$$F^{(2)} = (E^{2\omega})^* \otimes E^{\omega} \otimes E^{\omega} + \text{c.c.} \quad (41)$$

$$F^{(3)} = (E^{3\omega})^* \otimes E^{\omega} \otimes E^{\omega} \otimes E^{\omega} + \text{c.c.} \quad (42)$$

Equations 41 and 42 apply respectively to second- and third-harmonic generation. These tensors, when contracted with the corresponding optical susceptibilities (see section VI and eq 68 therein) drive the laser–matter energy exchange rate in a given nonlinear process. Their definition can be readily extended to all three-wave and four-wave mixing processes by adequate choices of frequencies. The $F^{(n)}$ tensors can be similarly decomposed in irreducible components, their relative angular positions with respect to β or γ, as shown in Figure 5, reflecting the efficiency of the field–matter nonlinear interaction process for a given set of polarizations. Similar considerations can be applied to multipoling:[1] the relevant couple of extensive and intensive tensors are then shown to be, in the context of generalized Langevin tensorial orientation, the multipolar charge distribution and the multipoling field distribution. These tensors may be fruitfully represented in a similar vectorial framework as proposed here for optical nonlinear interactions. As will be shown in section VI, parallel decomposition in irreducible components of $\chi^{(n)}$ and $F^{(n)}$ for $n = 2,3$ entails interesting results in terms of polarization behavior of interacting beams in a nonlinear medium.

We concentrate hereafter on so-called "planar" systems[18] whereby the β tensor is four-dimensional: whether the molecule is actually planar in the true geometric sense which may include irrelevant out-of-plane σ bonds, is not essential inasmuch as a 2-D β tensor, related to the conjugated portion of the molecule, applies.[18] Two sets of expressions have been worked out for the irreducible components of β, depending on the molecular environment: one may want to consider a planar molecule either as a truly 2-D confined system with interactions also confined to the plane or, more realistically, as a 2-D system embedded in 3-D spaces, i.e. allowing for out-of-plane Coulomb interactions betwen in-plane particles or out-of-plane intermolecular interactions as discussed in more details in Appendix D.

A simple and widely used reference model is that of a 1-D system[19] whereby β is limited to a single tensorial term, namely $\beta = \beta_{XXX} \boldsymbol{X} \otimes \boldsymbol{X} \otimes \boldsymbol{X}$, and $\boldsymbol{X}$ stands for the charge-transfer axis in p–nitroaniline-like chromophores. One may then derive the β tensor of the simplest corresponding octopolar molecule by mere tensorial addition of the β's of the individual 1-D component moieties arranged in a 3-fold planar arrangement of D_{3h} symmetry (see Figure 3). Such a purely geometric procedure, already referred to in section II, is based on the assumption that interactions between 1-D subsystems are negligible, obviously boundary situation corresponding to "weak" substituents or limited conjugation. Following this definition, P_2 (or P_3) will then correspond to C_2 (C_3) in the framework of Figure 5, where the C's stand for the β or $\chi^{(2)}$ tensor for 1-D systems and the P's to their "additive" octopolar D_{3h} counterparts, subscripts 2 and 3 reflecting the choice of a 2-D or 3-D representation. One may note that a 1-D rank-3 tensor is not purely dipolar but consists of both an octopolar and a dipolar component, hence the off-axis positions of the C's. In most interesting cases, and in particular for the pNA–TATB couple, the additive assumption is not valid since mutual interactions between the NO_2 and NH_2 groups in TATB will scramble individual pNA contributions.[7,8,16] The P point is then meant to serve as a reference position, its distance to the experimental or

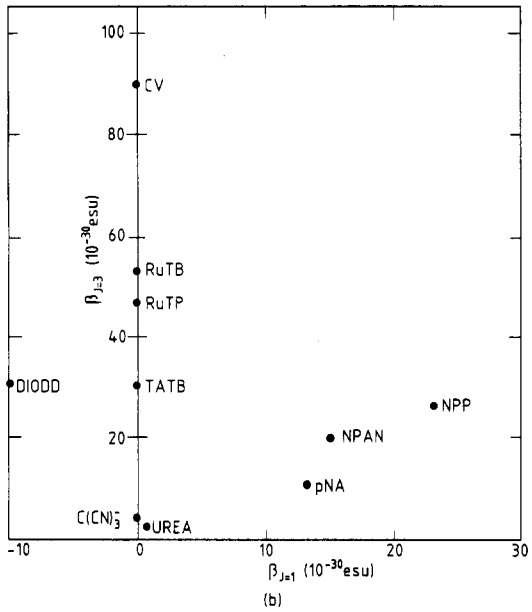

Figure 6. Various examples of molecular systems of mixed or purely octopolar nature with data originating from either experiments or theory are plotted according to the representation scheme in Figure 5a, namely: molecules already detailed in the caption of Figure 4; pNA;[7] tricyanomethanide ion;[27,28] TATB;[5,7] crystal violet (CV);[29] ruthenium(II) tris-(2,2'-bipyridyl) (RuTN) and ruthenium(II) tris(1,10-phenanthroline) (RuTP)[6] (data from an EHLS experiment and subsequent dispersion to zero frequency); 1,3,5-triphenyl-2,4,6-triazine (TPTR) (unpublished data from EHLS experiment). The dispersion of β magnitudes for pNA analogs may reflect the different types of calculation and corresponding approximations, but still points out to a fairly balanced $J = 1$ and $J = 3$ breakdown of β for this molecular family.

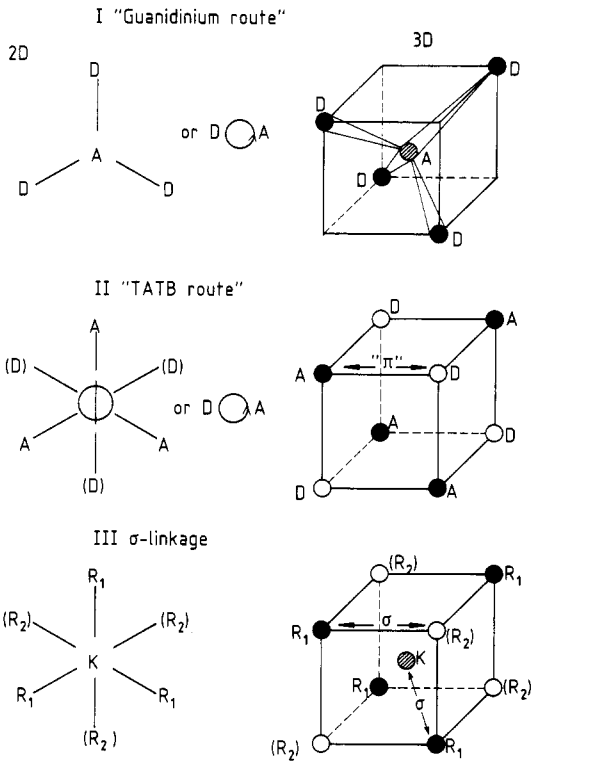

Figure 7. Various molecular engineering routes toward the optimization of the β susceptibilities of octopolar nonlinear molecules in both planar and nonplanar cases. Note that in all cases, the donors (D) can be permuted with the acceptors (A). In case II, either D or A can be omitted leading to trisubstituted TATB analogs. In case III, R_1 (or R_2) corresponds to a molecule of the sample type I (II), or to a dipolar molecule such as belongs to the paranitroaniline family. There again, R_1 or R_2 can be omitted.

computationally estimated $\beta_{J=3}$ component of the actual system being a measure of the amount of octopolar interaction in this system. In the case of pNA and TATB, as well as similar conjugated dipole–octopole couples, one would be entitled to refer to octopolar charge-transfer interaction.

Figure 6 depicts various molecular systems with data of either theoretical or experimental origin. Of particular interest is the inspection of the $J = 3$ axis (purely octopolar systems) which evidences that high β values can indeed be achieved with trigonal molecular systems as compared to the more classical pNA-like systems. Particularly noteworthy is crystal violet which can be viewed as a more extended and conjugated version of the guanidinium cation with the central carbon playing the role of an electron donor. While the $\beta_{J=1}$ component is available from the now well-documented EFISH experiment, the $\beta_{J=3}$ component has remained somewhat more elusive in this context owing to the absence of a permanently orientable dipole. The so-called elastic second-harmonic light scattering (EHLS) experiment demonstrated and analyzed by Maker, Terhune, and co-workers[30,31] had in fact provided the clue from the early days of nonlinear optics: carbon tetrachloride, a typical octopolar tetrahedral molecule with a single β_{XYZ} coefficient, had been fully characterized by this technique as early as 1964, with a full spectral and temperature analysis reported in ref 31. This experiment provides a combination of squared β coefficients weighed by factors reflecting correlation-induced statistical orientation. The noncoherent nature of the observed harmonic signal makes it proportional to the number of nonlinear molecules rather than to its squared value as results from coherent SHG, thus requiring a sensitive off-axis detection system. This technique is described in more detail in section V. Combination of EFISH and EHLS may provide, in some cases, additional relevant data such as the angle between the dipole moment and $\beta_{J=1}$ in systems where the octopolar contribution $\beta_{J=3}$ can be legitimately neglected (e.g. long-chain polyenes). Utilization of this technique has been reported in the context of neutral dipolar organic solutions.[32] EHLS has recently been used to estimate the octopolar nonlinearities of crystal violet (CV),[29] ruthenium trisbipyridine (RuTB), ruthenium trisphenanthroline (RuTP),[6] and tricyanomethanide[27,28] ions, with corresponding zero-frequency extrapolated values in Figure 6.

Various general 2-D and 3-D strategies toward the optimization of $\beta_{J=3}$ are displayed in Figure 7 and illustrated by somewhat more specific examples in Figure 8. The first one in Figure 7, based on a central acceptor atom interacting with surrounding donor moieties or vice versa in a trigonal arrangement, is inferred from the guanidinium cation. Such molecules as guanidine and trimethylenemethane had been at the origin of the concept of "Y-delocalization"[33] in the context of stability and reactivity. Its topological implications are reported in ref 34 and have naturally led to investigation of its more conjugated extension,

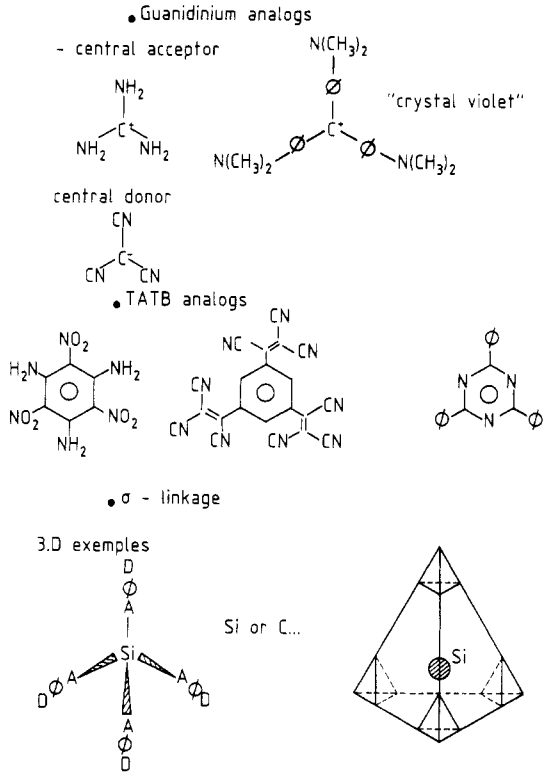

Figure 8. Specific examples of implementation of the engineering routes depicted in Figure 7.

namely the crystal violet cation.[29] Similarly, the fully planar tricyanomethanide anion can be viewed as an inverted guanidinium where the central atom and peripheral groups are now respectively donor and acceptor.[27,28] Whether the molecule is actually planar or not does not really matter provided its symmetry cancels the net dipole moment: comparable 3-D systems can be thought of with a more "heavy" central atom so as to allow for conjugation via higher order orbitals. The TATB route generalizes over the initial observation of a strong signal from TATB where the interaction between acceptor and donor groups is mediated by a conjugated system (an aromatic ring in the case of TATB). The conformation of TATB-like systems has been extensively studied[35,36] and shown to exhibit distorted boat structures. However, the highly connected intermolecular H-bonding network of TATB crystals keeps molecules in a perfectly planar structure as evidenced from the earlier structure determination by Cady and Larson.[16] Theoretical results on "inorganic benzenes" such as $B_3N_3H_6$ or $Al_3N_3H_6$ are reported in ref 37. A different, however interesting case is that where the central atom or moiety is just meant to orient type I and type II molecules, as well as pNA analogs, in an adequate octopolar assembly. This direction can be illustrated by four identical pNA-type molecules aligned along the direction of sp^3 tetragonally hybridized orbitals originating from a central binding silicon or carbon atom. Alternatively, four tetrahedral octopolar molecules, as also shown at the bottom of Figure 8, can be accommodated at the apex of a regular tetrahedron in a sort of "self-similar" octopolar arrangement held together by a central sp^3 binding atom or tetragonal moiety.

IV. Quantum Mechanical Considerations: From the Two-Level to a Three-Level Model

Modeling of the optically driven polarization properties of octopolar systems based on quantum mechanical approaches provides interesting insights onto the underlying excited states, transparency, polarized charge redistribution, and β magnitudes. It had been pointed-out at the origin of this work[1] that, regardless of the actual approximation level of quantum chemical descriptions of the octopolar system, the two-level quantum model all-pervadingly invoked for pNA analogs is irrelevant in the context of octopoles owing to the cancellation of all vectorial quantities including in particular $\Delta\mu$, the difference between excited- and ground-state dipole moments. We had instead proposed, as the simplest framework capable of accounting for octopolar quadratic nonlinearities, a three-level system, or a combination of these, whereby a nonzero β originates from the product of dipolar transition moments coupling the three states e.g. $\Sigma_u A_u \mu^u_{12}\mu^u_{23}\mu^u_{31}$, where the index u labels different sets of three level systems contributing to β and A_u is a frequency-dependent coefficient. Indeed, it turns out from mere inspection of character tables that trigonal groups, such as the D_{3h} group, specifically exhibit sets of E-labeled degenerate irreducible subspaces of dimension 2 that are reportedly playing a pivotal role in octopolar nonlinearities.[8] The character table of the basic trigonal C_3 group is indeed composed of the fully symmetrical A representation and of a doubly degenerate E representation with a similar pattern repeated in all-trigonal groups of interest here such as C_{3v}, C_{3h}, D_3, and D_{3h}.

The only dipole-allowed transition has to connect an A state to an E state within Hückel theory.[37] One may find in Vol. III of ref 37 detailed Hückel calculations on a variety of conjugated trigonal species such as the methylene–propenyl dication and diradical, the cyclopropenyl cation and anion diradical, and the triphenylmethyl cation and radical, all of D_{3h} symmetry. A common feature of the related spectroscopic calculations is the exclusively nE″ and nA″ assignment of occupied as well as unoccupied monoelectronic Hückel orbitals.

The situation is a bit more complex when singly and doubly excited configurations are introduced within the framework of Hartree–Fock theory:[8] the 1E′ and 5E′ doubly degenerate states are shown to be connected to the $1A'_1$ ground state and to participate to degenerate triangular pathways (i.e. $1A'_1 \rightarrow 1E'_a \rightarrow 1E'_b \rightarrow 1A'_1$ and related ones, where subscripts a and b label the two degenerate states in the 1E′ manifold). In addition, 1E′ and 5E′ states are mutually connected in regular triangular pathways such as $1A'_1 \rightarrow 1E'_a \rightarrow 5E'_b \rightarrow 1A'_1$. A full qualitative and quantitative discussion is to be found in ref 8 by Pierce et al., together with the accompanying β expression in a sum-over-state expansion for TATB. It is shown by Joffre et al.[8] that molecular and transition dipole symmetries are best matched in this context by circularly polarized light. Triply degenerate states might be involved, but only in the case of cubic symmetry (i.e. T_d symmetry) which has not been studied so far in this context from a theoretical standpoint.

Different types of calculations at different levels of approximation have brought some quantitative insights on some specific molecules and, in particular, helped evidence the expected appropriate three-level systems. Partially up to fully correlated Pariser–Parr–Pople π-electron calculations[8] offering the possibility of continuous tuning of side group donor or acceptor strengths via modulation of on-site energy terms allow for ensuing physical discussions of finite-field[38] as well as sum-over-state values of β. More specific calculations are reported in ref 7. In both cases, calculations consistently point out similar values for the β_{XXX} coefficient of *p*-nitroaniline (pNA) and that of TATB, which confirms the discussion started in section II: in general, the ratio of β magnitudes for two arbitrary polar or nonpolar molecules of C_{2v} symmetry or subsymmetry labeled by 1 and 2, is given by

$$\frac{\|\beta^1\|}{\|\beta^2\|} = \frac{\beta^1_{XXX}(1 + 3u_1^2)^{1/2}}{\beta^2_{XXX}(1 + 3u_2^2)^{1/2}} \qquad (43)$$

with $u_i = \beta^i_{XYY}/\beta^i_{XXX}$ and $i = 1, 2$. The main difference between pNA and TATB lies in the ratios u_i: while the anisotropy of polarizability is strong in the case of pNA, making the parameter $3u^2$ almost negligible with respect to 1 in eq 43, u is exactly equal to -1, as from D_{3h} symmetry, in the case of TATB. This gives a strong advantage, at almost equal β_{XXX} value, to octopolar over corresponding dipolar species, the origin of the factor of 2 almost gained thereby becoming clear from eq 43. Furthermore, the excited-state charge distribution and dipolar transition moments of TATB resulting from the sum-over-state approach evidence a more intricate mixture of states, blurring any clear assignment to charge-transfer states of para and ortho nature.

In the PPP calculations reported in ref 8, the on-site energy of carbon atoms in the benzene ring is modified by an amount Δ with sign and magnitude reflecting the nature (positive Δ for a donor versus negative Δ for an acceptor) and strength of the substituent. The norm of β is displayed in Figure 9 as a function of Δ for para-substituted (a) and hexasubtituted (b) benzene molecules. Calculations were performed at different approximation levels ranging from Hückel to full CI. In agreement with trends already reported for dipolar systems,[39] octopolar molecules exhibit as well an optimal Δ value, however of smaller magnitude than in the dipolar case. The effect of electron correlation is seen to affect considerably the nonlinearity: for all but the largest values of Δ, where the adequacy of the model is questionable, inclusion of electron correlation lowers the predicted norm of β. More realistic calculations have also been reported in ref 8, where all π electrons and atomic sites, except for the hydrogenes, are accounted for within the framework of an extended PPP formalism. A consistent series of corresponding dipolar and octopolar molecules has thus been investigated via this scheme with main results summarized in Table 2 and Figure 10. A striking feature is the consistent increase of β magnitudes as well as absorption energies when moving from a dipolar to the corresponding octopolar species (e.g. from pNA to TATB). This trend is rationalized in Figure 10b which compares energy levels and optical transition schemes of benzene

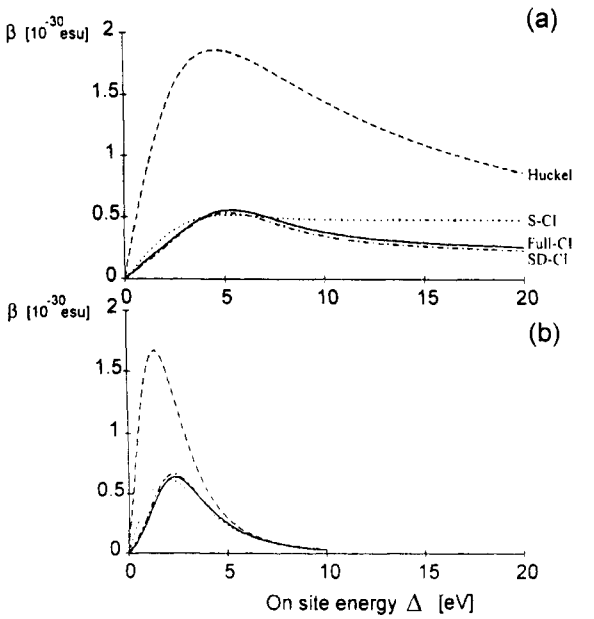

Figure 9. Calculation of the norm of β using the sum-over-states method, as from ref 8, for (a) the para-substituted benzene ring and (b) the octopolar hexasubstituted ring. The approximations used are Hückel (dashed line), single CI (dotted line), double CI (dot–dashed line), triple CI (double dotted–dashed line), and full CI (solid line).

Table 2. Components of β Obtained at the SD-CI, Finite-Field Level[a]

	$\lvert\beta^{dip}\rvert$	$\beta^{dip}_{xyy}/\beta^{dip}_{xxx}$	$\beta^{dip}_{J=3}/\beta^{dip}$	$3\beta^{dip}_{J=3}$	β_{oct}
NH_2	0.41	0.01	0.48	0.60	0.64
NO_2	1.21	0.21	0.17	0.62	1.17
$NO_2 + NH_2$	2.28	0.08	0.37	2.53	3.31

[a] β_{dip} (or β_{oct}) refers to dipolar (octopolar) molecules (e.g. aniline and 1,3,5-triaminobenzene, etc.) with $\beta^{dip}_{J=3}$ corresponding to the octopolar component of β_{dip}. This increasing discrepancy between the two last columns ($3\beta^{dip}_{J=3}$ and $\beta_{oct} = \beta^{oct}_{J=3}$) reflects the departure from a perturbative model whereby β_{oct} would result from mere tensorial addition of dipolar nonlinearities respectively oriented at 0, 120°, and 240°. In the case of TATB, (i.e. NH_2, NO_2 as substituents), mutual interactions between the various sites strongly differentiate its nonlinear behavior from that of an additive trigonal extension of pNA whereas the moderate substitution pattern in 1,3,5-trianiline is consistent with the additive scheme from aniline.

to that of dipolar and octopolar systems. In highly symmetric benzene systems, stringent selection rules impose $\Delta m = \pm 1$ for optically connected states, following D_{6h} group notations with m standing for the component of the orbital angular momentum along the C_6 axis. This condition precludes the closure of a triangular coupling scheme which would be required to sustain a nonzero β tensor, not surprisingly in agreement with the noncentrosymmetry constraint. In contrast with benzene, dipolar systems may be viewed as weakly symmetric systems with less binding symmetry constraints, if at all, thus allowing for different triangular coupling schemes corresponding either to two-level or three-level transitions (respectively in full and dotted lines in Figure 10b). Octopolar systems stands at an intermediate level of symmetry which permits viable triangular coupling schemes: these correspond either to doubly degenerate E_u states, which are specific of trigonal symmetry, or to nondegenerate three-level system (respectively in full and dotted lines in Figure 10b). The benefit in terms of efficiency–transparency

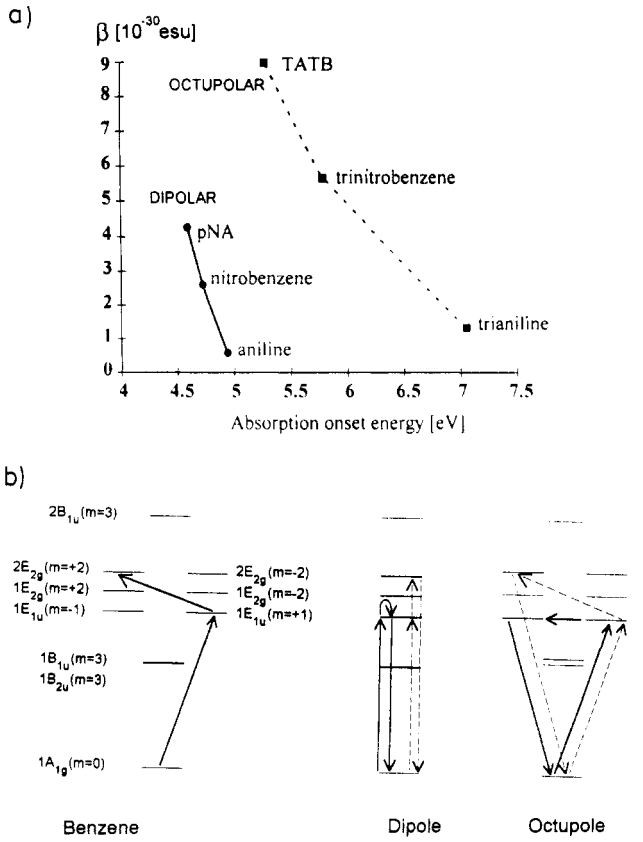

Figure 10. Displacement of the efficiency–transparency tradeoff is evidenced in (a) where the absorption energy and β magnitude of corresponding dipolar and octopolar moieties are compared. The lower energy states of benzene and dipolar and octopolar molecules calculated at single CI level for Δ = 1 eV are represented in (b) together with various optical coupling schemes underlying β. Dotted lines correspond to nondegenerated three-level coupling scheme and solid lines to degenerated three level or the usual two-level scheme. The absorption blue shift in a may be accounted for by tighter selection rules in the case of octopoles, as opposed to dipoles, whereby the low-lying B_u state is not accessible from the ground state.

tradeoff, when increasing the symmetry constraints from dipolar to octopolar systems, originates from the different selection rules governing the coupling of the ground to the low-lying B_u state(s). Whereas these states do not contribute to the nonlinearity in either case, the transition is permitted for dipolar systems, thus leading to absorption without the benefit of β enhancement, while being forbidden for octopolar systems, hence a blue shift. From calculations in ref 8, β magnitudes (or absorption energy onset) increase from 4.26 (4.6) to 9 10^{-30} esu at (5.2 eV) when going from pNA to TATB.

It is thus proposed that the efficiency–transparency tradeoff for nonlinear molecules can be favorably displaced by replacing dipolar engineering schemes by corresponding octopolar ones.

V. Harmonic Light Scattering in Octopolar Solutions: Experimental Determinations

A. Motivations

In contrast with theoretical studies, molecular scale experimental investigations, such as performed in solution by the EFISH technique,[40] have been so far precluded by the very absence of molecular dipole moment. In the traditional EFISH scheme, poling of the chromophores in solution is ensured by the dipolar coupling energy $-\vec{\mu}\cdot\vec{E}_p$ where $\vec{\mu}$ is the molecular ground-state dipole and $\vec{E}_P$ the applied DC poling field. Such a scheme is forbidden for octopolar dipolarless species, at least for a constant vectorial field distribution such as obtained at the center of an electroded cell with planar capacitors. The so far almost exclusive focusing of molecular engineering research on dipolar systems has obviously been biased by the symmetry bottleneck imposed by the traditional EFISH setup: one will naturally tend to design molecules inasmuch as measurable, thus priviledging dipolar molecules compatible with the poling requirement. The outcome of the EFISH experiment is furthermore reduced to the sole $\beta_{J=1}$ component, out of a potentially richer, however largely elusive, β-tensor rotational spectrum. Resorting to an octopolar poling field distribution, by way of extension of previously reported quadrupolar measurement schemes,[41] has been proposed,[3] but entails difficulties due to inhomogeneity of the octopolar field and exponentially decreasing "multipoling" efficiency as a function of the multipolar order of interest.

The approach followed here relies on harmonic light scattering (HLS), as initially proposed and developed by Terhune and Maker.[30,31] This experiment and related ones, such as hyper-Raman scattering, are reviewed in ref 42. This technique has been recently applied to solutions of nonlinear organic molecules.[32] Due to incoherent light harmonic scattering, sometimes referred to as the hyper-Rayleigh process,[32,42] harmonic light can be detected and its intensity shown to be proportional to N (number of nonlinear scatterers) and to the averaged value of the rank 6 tensor $\beta \otimes \beta$, the averaging conditions depending on the structure (solution, polymer, or crystal) of the medium. The even rank 6 of $\langle \beta \otimes \beta \rangle$ guarantees a nonzero value, even in a centrosymmetric medium, in contrast to the "squared" rank-3 $\langle \beta \rangle^2$ tensor underlying usual coherent SHG processes. This HLS experiment entails a double benefit, specific of this study: The first one is the possibility, in the absence of a poling field, to perform measurements on charged species. The additional one is the possibility to access to β determination of dipolarless molecules, such as octopolar nonlinear species, where external field poling is irrelevant.

In the subsequent experimental investigation, the relevance of HLS experiments, as an alternative to EFISH, toward the measurement of octopolar nonlinearities is outlined and a new type of octopolar nonlinear molecules based on the so-called "central-atom" strategy is evidenced. Instead of a central π-electron reservoir mediating charge-transfer interactions between peripheral electroactive side groups such as TATB analogs, a donor (or acceptor) group or atom is the central cornerstone of the molecular structure, with three accepting (donating) groups laterally grafted in a 3-fold D_3 or D_{3h} symmetry octopolar arrangement (depending on the out-of-plane twisting of the side groups). Such generic structure has been obviously inspired by guanidinium, a well-known, readily available trigonal cation, whereby three lateral electron-donating amino groups interact with a central charge-defective,

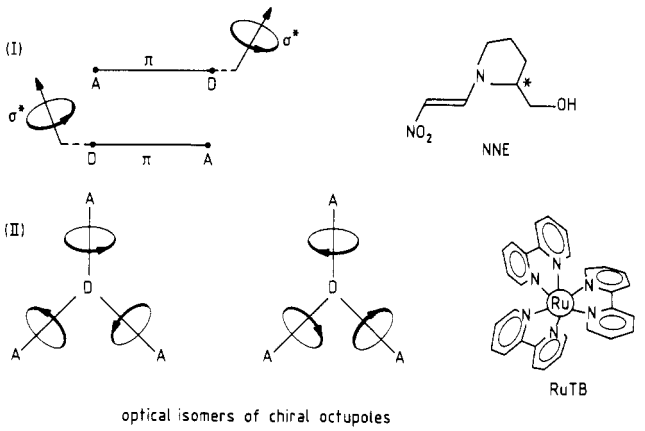

Figure 11. Two different schemes aiming at the combination of chirality and intramolecular charge transfer features. In the more classical approach (part I) a σ-type chiral moiety is attached to π-conjugated donor–acceptor molecule. Antiparallel coupling of the π moieties of neighboring molecules, in keeping with a noncentrosymmetric arrangement of the σ chiral portions, may lead to a quasicancellation of the overall nonlinearity of the bimolecular system. In part II, chirality originates from (+) or (−) torsion angle of the polar peripheral branches of an octopolar trigonal charge-transfer molecule or ion with a central donating (or alternatively accepting) group. In part II, chirality and charge-transfer features are intimately associated, in contrast with part I.

hence electron-accepting, carbon atom.[43] A similar structure, where the central atom is a donor surrounded by three acceptor groups, can also be implemented, with a C^- electron-rich, hence donating central atom interacting with three cyano accepting groups.[27,28] This "central-atom" strategy is applied to a quasiplanar ionic system exhibiting a quasi-D_{3h} symmetry, crystal violet (CV) (see Figure 8). As for guanidinium ions, the central atom is a positively charged electron-accepting carbon atom, linked to three conjugated dimethylanilino donor groups.

Another illustration of this central atom route is also provided in the following by three-dimensional, D_3-symmetry metal complexes, exhibiting the additional advantage of a chirality directly associated to the electronic charge transfer.[6] Molecules that have been reported, namely tris(2,2′-bipyridyl)ruthenium(II) bromide hexahydrate (RuTB) and the parent tris(1,10-phenanthroline)ruthenium(II) chloride hexahydrate (RuTP), are meant to combine the benefits of a metal-to-ligand charge transfer (MLCT) contributions to β,[44] together with an "inherently" chiral geometry. In usual nonlinear chiral molecules,[21,25,45-46] the charge-transfer-sustaining π moiety (e.g. a substituted benzene ring) is electronically disconnected from the remaining σ chiral portions. Such a typical construction is found in methyl[(2,4-dinitrophenyl)amino]propanoate (MAP)[25] or *N*-(4-nitrophenyl)-L-prolinol (NPP).[21,45] Although these two specific examples illustrate successful attempts to induce crystalline non-centrosymmetric and even optimized structures, it falls short, in many instances, of guaranteeing a strong nonlinearity.[46] The main shortcoming of this type of molecular design is sketched in Figure 11: in such a bimolecular association, actually found for example in 2-(*N*-prolinyl)-1-nitroethylene (NNE),[46] the conjugated π-electron charge-transfer systems, which bear no (or only indirect) chiral features, may set up a quasi-antiparallel geometry, thus cancelling the major part of β, whereas the chiral σ groups, which do not contribute significantly to the nonlinearity, may form an oriented sublattice, however of limited relevance for nonlinear optics.

A different molecular design scheme whereby the β-sustaining charge-transfer system itself would be made chiral, could thus avoid this drawback. RuTB and RuTP exhibit both structural and electronic features, which combine chirality as a result of a D_3 symmetry propeller geometry, and MLCT charge-transfer potential in an octopolar nonlinear arrangement of the "central-atom" type.

B. Structure and Electronic Spectra of Octopolar Molecules

1. Crystal Violet

Para-substituted triphenylmethanes form a well-known class of dyes discovered one century ago and widely used for their high tinctorial strength. Among these, crystal violet (CV) displays a D_3 symmetry associated with three intramolecular charge transfers (ICT) from the dimethylamino donor groups toward the central electron-defective carbonium moiety through the phenyl rings. The CV molecule is sketched in Figure 8.

Triphenylmethane dyes cannot adopt a fully planar conformation: on the basis of crystallographic studies,[47] the expected geometry of CV is that of a D_3 symmetric propeller. The equilibrium geometry of the isolated molecule has been calculated using intermediate neglect of differential overlap (INDO) molecular orbital calculations,[48] which results in a three-bladed propeller where the three aromatic rings are twisted out of the molecular plane by about 30°. It has been suggested by various authors[49-50] that in solution, two rotational isomers of CV with D_3 and C_2 geometry respectively, could coexist. This assumption may however be discarded by consideration of the torsional energy required to transform the CV molecule from its dipolarless D_3 configuration into the C_2 polar configuration. Such energy (of the order of 5000 cm^{-1}) is large compared to kT at room temperature, whereas the interconversion barrier between the two forms (of the order of 10 000 cm^{-1}) is twice as large.[48] This precludes the existence of a C_2 form in the ground electronic state.

The situation is however more complex in the excited state: the visible spectrum of CV in acetone (Figure 12a) consists of two overlapping bands, the most intense being in the red ("R band") and the less intense in the blue ("B band") spectral region. This factor could indicate solvent-induced symmetry breaking of the CV molecule in the excited state, leading to a lifting of the degeneracy of the excited electronic states expected for the trigonal D_3 ion. Furthermore, INDO calculations as well as Raman studies show that breaking the degeneracy of the electronic transition does not affect the D_3 symmetry of the ground state of CV.[48] R and B bands are then believed to result from solvent-induced symmetry breaking of a degenerate excited state, whereas the 3-fold symmetry of the ground state would remain unchanged.

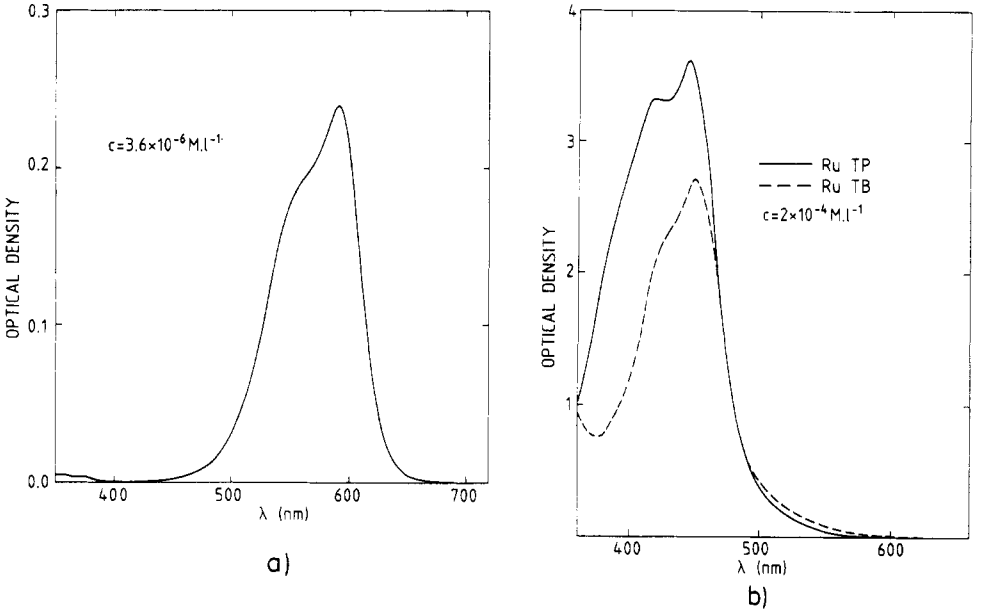

Figure 12. Absorption spectrum of crystal violet in acetone (a) (concentration 3.6×10^{-6} M) and of RuTP (full line) and RuTB (dashed line) in ethanol (b) (concentrations 2×10^{-4} M).

2. Ruthenium Derivatives

Although there still does not yet exist an unambiguously correct assignment of either the electronic absorption or the luminescence spectrum for RuTB or RuTP, the main visible absorption band (around 450 nm) can be assigned to a d $\rightarrow \pi^*$ metal–ligand charge-transfer (MCLT) transition. In the electronic ground state, the splitting of the five degenerate levels of the 4d electrons under D_3 symmetry leads to a doubly degenerate e(d) and an a_1 level. The MLCT excited state of the complex is viewed as a Ru^{III} d^5 core, the excited electron being described by the ψ^* orbital of the π^* system of the ligands. Visible absorption spectra of RuTB and RuTP are displayed in Figure 12b. They are clearly dominated by an intense absorption band around 450 nm originating from the d $\rightarrow \pi^*$ metal–ligand charge-transfer transition. The structure of this band originates from transitions located respectively at 449 nm (i.e. 22 272 cm^{-1}) and 422 nm (i.e. 23 697 cm^{-1}) for RuTB. This energy splitting of the main MLCT transition results, according to ref 51, from a weak interligand coupling separating the energy level of the first excited state ψ^* orbital into two separate levels labeled as $a_2(\psi^*)$ and $e(\psi^*)$. The lowest (or the highest) transition can be assigned to a e(d) $\rightarrow$ a_2(d) (e(d) $\rightarrow$ e(ψ^*)) electronic transition.

An essential structural difference with crystal violet, besides the presence of a metallic central electron-donating ruthenium atom, is the frozen propeller geometry of RuTB and RuTP as opposed to the more flexible link between the central C^+ atom and connected phenyl rings of CV. Such possible twisting precludes chirality in the case of CV and related triphenylmethanes; furthermore, earlier attempts to design organometallic systems for quadratic nonlinear optics were mainly using metal atoms as replacement of donor or acceptor side groups[44,52,53] in a polar geometry, thus essentially following the lines of the paranitroaniline blueprint. Octopolar nonlinear structures allow one to locate the metal atom in a more strategic position at the center of the charge transfer system, thus possibly making a better use of the d orbital hybridization schemes in an organic ligand environment. It is believed that such a multiple substitution scheme is better adapted to "exhaust" (and eventually saturate) the nonlinear reservoir made up by the electron-rich polarizable shells of metals or transition elements, in contrast with the less demanding traditional unipolar substitution.

3. Resonances

It must be pointed out that the harmonic frequency of the Nd^{3+}:YAG laser used in the harmonic light scattering (HLS) experiment ($\lambda = 0.532$ μm) is located within the electronic absorption band of CV and ruthenium derivatives as shown in Figure 12. In the case of crystal violet, the energy of the second-harmonic generation of the Nd^{3+}:YAG laser lies beyond the maximum absorption wavelengths λ_{max} of the two electronic transitions in the visible. If the classical two-level model used for most nonlinear dipolar molecules[40] were applied here, $\beta(-2\omega;\omega;\omega)$ would be expected to be of the opposite sign with respect to its corresponding "static" value at zero frequency $\beta(0)$. The two-level model is however obviously not valid in the present case of octopolar molecules, as it would lead to a strictly vanishing β as a result of the symmetry cancellation of ground as well as excited state dipolar moments. A three-level model has been proposed instead,[1,8] and its implications as to the sign of β will be discussed in more details elsewhere. If furthermore one considers, as proposed in ref 8, a three-level system made up of the ground state and of a doubly degenerate excited state (typical of trigonal systems as from group representation theory), the dispersion behavior of the related β can be shown to be similar to that of a classical two-level system. The expression of β, within such a model, is strikingly similar to that of a two-level system, namely:[8]

$$\beta = \frac{3}{2}\frac{|\mu_{01}|^2\mu_{11}}{E_{01}^2}\frac{E_{01}^2}{(E_{01}^2 - 4\hbar^2\omega^2)(E_{01}^2 - \hbar^2\omega^2)} \quad (44)$$

where $\mu_{1\bar{1}}$, the transition dipole moment connecting the degenerate state $|1>$ to its counterparts $|\bar{1}>$, replaces the difference $\Delta\mu = \mu_{11} - \mu_{00}$ between excited- and ground-state dipole moments met in the usual two-level expression. In expression 44, the label 0 corresponds to the ground state and E_{01} is the energy difference between the degenerate excited states and the ground state. We will thus report, in the following, resonantly enhanced $\beta(-2\omega;\omega;\omega)$ values measured at 1.064-μm fundamental wavelength. The sign of β or $\beta(0)$ cannot be experimentally ascertained using the HLS experiment.

C. Experimental Setup

HLS provides a unique technique for β measurement of nondipolar and/or ionic molecules, which are out of reach of the standard electric-field-induced second-harmonic (EFISH) generation technique. The absence of a permanent dipole moment to be coupled to a DC electric field so as to pole the solution makes EFISH irrelevant. Furthermore, the presence of ionic species in a solution precludes the application of a poling electric field. The combination of these two features, absence of dipole and ionic nature, designates CV as an ideal candidate for β measurement in solution by use of HLS technique, where no application of an external electric field is required. HLS was proposed and used first by Terhune and Maker[30-31] as a measurement technique of β values; this method requires high peak power fundamental pulses and an efficient collection system of harmonic scattered photons. The experimental setup, similar, in its principle, to that used by Maker in ref 31, is sketched in Figure 13. A transverse and longitudinal single-mode Nd^{3+}:YAG laser is used as the fundamental source, consisting of 10-MW peak power, 10-ns duration IR pulses at 1.064 μm (repetition rate 10 Hz). The incident IR intensity can be continuously monitored by a set of two half-wave plates and crossed Glan polarizers. A small part of the incident beam is removed by a glass plate and sent toward an IR-sensitive photomultiplier, providing the "reference" fundamental intensity to which the harmonic one will be compared. The main fundamental beam is focused into the sample using a 20-cm focal length converging lens. The sample consists in an adequately designed parallelepipedic spectrophotometric cell, presenting five polished windows so as to allow for simultaneous longitudinal illumination and transverse collection of the scattered emission. Solutions of increasing concentrations of the molecules to be measured in acetone are preliminarly cleaned through 0.5-μm Millipore filters in order to remove most microscopic particles which could otherwise induce breakdowns in the presence of the focused IR laser beam. In the case of CV molecules, very low concentrations, ranging from 2×10^{-6} to 10^{-5} M, are used, in order to avoid strong signal reduction due to the linear absorption of the second harmonic light by CV molecules. Here the decrease of $I^{2\omega}$ due to linear absorption ($\epsilon = 33\,000$ cm^{-1} M^{-1} L at 0.532 μm) does not exceed 30% as compared to the fully transparent regime. Mixtures of CCl_4 and acetone in various volume ratios $r = V_{acetone}/V_{CCl_4}$ ($0 < r < 1$) and solutions of increasing concentrations of NPAN (2.10^{-3} to 10^{-2} M) in acetone, have also been considered for the sake of calibration. Assuming $\langle\beta^2\rangle = \langle\beta^2_{vec}\rangle$ for NPAN, the value $\langle\beta^2\rangle^{1/2} = 23$ for this compound was used for solvent calibration.

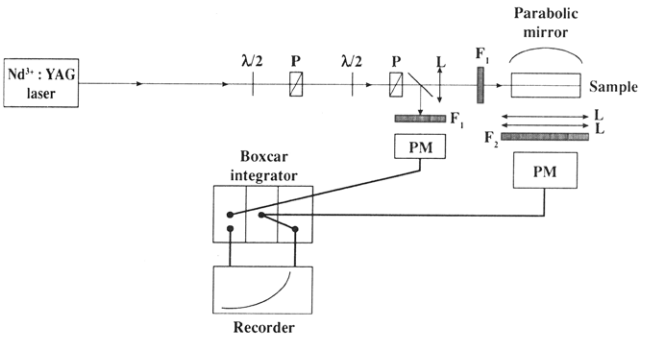

Figure 13. Experimental setup for the HLS experiment at 1.064 μm: $\lambda/2$, half-wave plates, P, glan polarizers; L, converging lens; F_1 (or F_2), filters selecting the fundamental (harmonic) photons; PM, photomultiplier. In the insert the laboratory axes X, Y, Z, along with the polarization direction of the fundamental beam, are indicated.

Collection of the scattered harmonic photons is performed in the transverse off-axis 90° direction, using a large (diameter 60 mm) and short focal distance (f = 50 mm) spherical lens associated to a less converging one (f = 70 mm) in order to focus the light onto the photocathode of a photomultiplier tube. In addition, a concave mirror (diameter 50 mm, f = 40 mm), set at the symmetric off-axis direction, helps to collect the light scattered on the side opposite to the photodetector, and therefore increases the signal-to-noise ratio by an average factor of 2. The harmonic beam is then spectrally filtered out by a Schott interference filter of 4-nm bandwidth.

It must be pointed out that the incident intensity of the fundamental beam must be kept at a relatively moderate level, owing to possible competing contributions of third-order nonlinear effects (among them Brillouin scattering and self-induced (de)focusing) that may significantly alter the expected quadratic dependence of the second-harmonic intensity $I^{2\omega}$ as a function of I^{ω}. $I^{2\omega}$ departs from its quadratic I^{ω} dependence for high fundamental intensity values (around 200 MW cm^{-2}), leading to a subquadratic behavior and a subsequent underestimated value of the scattering, probably as a result of nonlinear defocusing processes in the solution.

The reference fundamental signal and harmonic signal photons detected by photomultiplier tubes are processed in a Stanford Research System boxcar, sampled, averaged, and then recorded on an XY table, giving $I^{2\omega}$ as a function of I^{ω} or $(I^{\omega})^2$. The quadratic dependence of $I^{2\omega}$ versus I^{ω} is clearly evidenced in Figure 14 for a 10^{-2} M solution of NPAN in acetone.

D. Symmetry Considerations in HLS Experiment

The theory of second-harmonic light scattering in liquids has been developed by various authors,[31,54-56] assuming that molecular sites and sample dimensions are respectively negligible and significantly larger than the harmonic wavelength. The scattering process originates from fluctuations of induced molecular dipoles proportional to the square of the optical electric field E^{ω}, as a result of molecular electronic potential anharmonicity. Following the treatment by Terhune et al.,[30] the second-harmonic intensity is obtained from

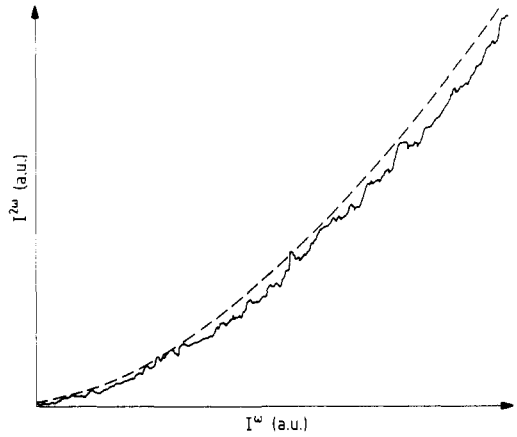

Figure 14. Experimental (full line) and expected quadratic (dashed line) variation of the scattered second harmonic intensity $I^{2\omega}$ as a function of the fundamental intensity I^{ω} for a 10^{-2} M solution of NPAN.

the "scattering tensor":

$$I_{ij}^{2\omega} = \frac{(2\omega)^4}{c^4 R_0^2} \int \langle d_{ikl,1}(-2\omega,\omega,\omega) d^*_{jmn,2}(-2\omega,\omega,\omega) \rangle \, d\upsilon \int E_k(\omega) E_l(\omega) E^*_m(\omega) E^*_n(\omega) \, dV \quad (45)$$

where 1 and 2 refer to two different molecules, and tensorial summations are implicitely performed over repeated indices.

In isotropic media the average value of d_{ikl} is zero. It is assumed in (45) that values of d_{ikl} at two different points are correlated only over distances small compared to a wavelength. The second harmonic intensity is then proportional to

$$\int \langle d_{ikl,1} d^*_{jmn,1} \rangle \, d\upsilon \quad (46)$$

Assuming that scattering units are randomly oriented, $I^{2\omega}$ may then be expressed as

$$I^{2\omega} = GN \sum_{ijklmn} \langle \beta_{ijk}(-2\omega;\omega,\omega) \beta^*_{lmn}(-2\omega;\omega,\omega) \rangle (I^{\omega})^2 \quad (47)$$

where N is the molecular density, G is a factor incorporating a local field correction, and β is the quadratic hyperpolarizability of individual molecules. G is given by

$$G = \frac{2^{11}\pi^5}{cR^2\lambda^4} \frac{n_{2\omega}^2 + 2}{3} \left(\frac{n_{\omega}^2 + 2}{3} \right)^2 \quad (48)$$

where the local field correction follows the Lorentz–Lorentz model and R is the distance from the cell to the harmonic detector, the dimension of the cell being small with respect to R.

In a configuration whereby the fundamental beam is polarized along Z, the harmonic signal is detected at 90° off the main propagation axis with an analyzer at 2ω along Z (see insert in Figure 13). Equation 47 reduces to

$$I_Z^{2\omega} = GN \langle \beta^2_{ZZZ} \rangle (I^{\omega})^2 \quad (49)$$

In a similar configuration, but with an analyzer at 2ω along X, the detected harmonic intensity is given by

$$I_X^{2\omega} = GN \langle \beta^2_{XZZ} \rangle (I^{\omega})^2 \quad (50)$$

In the case of unpolarized observation, the overall detected harmonic intensity is obtained by summation of (49) and (50):

$$I^{2\omega} = GN[\langle \beta^2_{ZZZ} \rangle + \langle \beta^2_{XZZ} \rangle](I^{\omega})^2 \quad (51)$$

The averaging is performed using product of the direction cosines between macroscopic and microscopic axes over all directions, assuming an isotropic fluid.

In the case of a mixture of two different species 1 and 2, the following expression is to be used:

$$I^{2\omega} = G(N_1 \langle \beta_1^2 \rangle + N_2 \langle \beta_2^2 \rangle)(I^{\omega})^2 \equiv k(I^{\omega})^2 \quad (52)$$

Equations 49 and 50 are then readily extended for a solution of two species. In the case of weakly absorbing media (total absorption losses less than 30%), the linear absorption at the harmonic wavelength can be taken into account in the following form:

$$I^{2\omega} = G(N_1 \langle \beta_1^2 \rangle + N_2 \langle \beta_2^2 \rangle) 10^{-\epsilon^{2\omega} c_2 l} (I^{\omega})^2 \quad (53)$$

where $\epsilon^{2\omega}$ is the molar extinction coefficient of the nonlinear molecule (species two) at the harmonic frequency 2ω, c_2 the concentration of species two, and l the effective pathlength. The solvent is assumed to be transparent within the harmonic frequency range. It must be pointed out that this expression holds—approximately—only for weak absorption losses. For stronger absorption regimes, the molar absorption coefficient must be introduced in the nonlinear propagation equations.

The averaged $\langle \beta^2 \rangle$ value of the rank-6 tensor $\beta \otimes \beta$ will depend on the symmetry of the molecule, whereas polarization of the fundamental and the presence or absence of an analyzer at the harmonic wavelength will determine the $\beta \otimes \beta$ coefficient to be averaged. The present experimental conditions, as shown in the insert of Figure 13, require only the calculation of $\langle \beta^2_{XZZ} \rangle$ and $\langle \beta^2_{ZZZ} \rangle$. A general method for the calculation of $\langle \beta^2_{IJK} \rangle$ terms has been proposed by Cyvin et al.[55] Following this approach, $\langle \beta^2_{ZZZ} \rangle$ and $\langle \beta^2_{XZZ} \rangle$ may be expressed in general as linear combinations of five basic quadratic polynomial expressions depending on β_{ijk} coefficients expressed in a molecular reference frame, namely:

$$\sum_i \beta^2_{iii}, \quad \sum_{i \neq j} \beta_{iii}\beta_{ijj}, \quad \sum_{i \neq j} \beta^2_{iij}, \quad \sum_{cyclic} \beta_{ijj}\beta_{jkk}, \quad \text{and } \beta^2_{ijk}$$

where the fourth term, corresponding to "cyclic" summation, is given by

$$\beta_{xxy}\beta_{yzz} + \beta_{yyz}\beta_{zxx} + \beta_{zzx}\beta_{xyy}$$

We report, in Table 3, the simplified expressions for these five quadratic polynomials in the case of molecular point-group symmetries encountered in this study. D_3 (or D_{3h}) correspond to a nonplanar, propeller-shape (planar trigonal) CV geometry. C_{2v} and T_d are the point groups of acetone and CCl_4, used respectively as solvent and for calibration in the subsequent measurements.

In Table 3, we have further assumed for D_{3h} and C_{2v} that z-containing β coefficients are discarded, in keeping with the assumption that out-of-plane nonlinearities are negligible with respect to in-plane ones (see the 2-D model in ref 19). Such considerations on the relative magnitude of β coefficients, as linked to specific electronic charge-transfer considerations, are not in contradiction with a lower symmetry (namely D_3) for

Table 3. Expressions of the Five Basic Quadratic Polynomial Expressions Used in the Averaging Procedure of $\langle\beta^2_{ZZZ}\rangle$ and $\langle\beta^2_{XZZ}\rangle$, for Various Point Groups Corresponding to Solvent and Solute Molecules Considered in This Series of Experiments

	D_3	D_{3h}	C_{2v}	T_d
$\sum_i \beta^2_{iii}$	β^2_{yyy}	β^2_{yyy}	β^2_{yyy}	0
$\sum_{i=j} \beta_{iii}\beta_{ijj}$	$\beta_{yyy}(\beta_{yzz} - \beta_{yyy})$	$-\beta^2_{yyy}$	$\beta_{yyy}\beta_{yxx}$	0
$\sum_{i=j} \beta^2_{iij}$	$\beta^2_{yyy} + 2\beta^2_{yzz}$	β^2_{yyy}	β^2_{yxx}	0
$\sum_{cyclic} \beta_{iij}\beta_{jkk}$	$-\beta_{yyy}\beta_{yzz}$	0	0	0
β^2_{ijk}	β^2_{xyz}	0	0	β^2_{xyz}

Table 4. Decomposition Factors of the Averaged Expressions of $\langle\beta^2_{ZZZ}\rangle$, $\langle\beta^2_{XZZ}\rangle$, and $\langle\beta^2\rangle = \langle\beta^2_{ZZZ}\rangle + \langle\beta^2_{XZZ}\rangle$, in Terms of Molecular Hyperpolarizability Coefficients for the Various Presently Relevant Point Groups (Respectively First, Second, and Third Term in Each Box)

	D_3	D_{3h}	T_d	C_{2v} (planar)
β^2_{yyy}	8/35, 16/105, 8/21	8/35, 16/105, 8/21	0	1/7, 1/35, 6/35
β^2_{yxx}	0	0	0	9/35, 11/105, 38/105
$\beta_{yyy}\beta_{yxx}$	0	0	0	6/35, -2/105, 16/105
β^2_{yxx}	18/35, 22/105, 76/105	0*	0	0*
β^2_{xyz}	12/35, 8/35, 4/7	0	12/35, 8/35, 4/7	0

[a] The starred zeros correspond to cancellations due to the assumed 2-D nature of the molecular hyperpolarizability tensor whereas unstarred ones result strictly from symmetry considerations. The axis labeling for the C_{2v} ($mm2$) group is not standard to allow for coherence between the various molecular symmetry types of interest in this study: the y axis is along the 2-fold axis (as opposed to the usual z notation) and the molecular plane is xy, in keeping with the choice for D_3 and D_{3h} molecules.

the overall molecular configuration. A well-known example is that of nonplanar pNA-like systems, such as NPAN,[23] where the π-conjugated subsystem is planar and hence β is satisfactorily accounted for by a 2-D tensor. Combining these polynomial expressions with standard coefficients as tabulated by Cyvin et al.[55] (see expressions 11 and 12 therein), leads to the desired expressions of $\langle\beta^2_{XZZ}\rangle$, $\langle\beta^2_{ZZZ}\rangle$, and their sum $\langle\beta^2\rangle = \langle\beta^2_{XZZ}\rangle + \langle\beta^2_{ZZZ}\rangle$, as summarized in Table 4 for the various molecular point groups of interest therein.

Application of Table 4 corresponds, in the case of unpolarized observations, to

$$\langle\beta_{D_3}{}^2\rangle = 8/21\ \beta^2_{yyy} + 76/105\ \beta^2_{yzz} + 4/7\ \beta^2_{xyz} \quad (54)$$

for D_3 symmetry, typical of RuTB and RuTP molecules.

The D_{3h} expression is simply obtained with the D_3 one by simply canceling z-containing coefficients then leading to

$$\langle\beta_{D_{3h}}{}^2\rangle = 8/21\ \beta^2_{yyy} \quad (55)$$

Contributions to HLS from a lowering of the D_{3h} symmetry constraints down to the D_3 symmetry group originate from

$$\langle\beta_{D_3}{}^2\rangle - \langle\beta_{D_{3h}}{}^2\rangle = 76/105\ \beta^2_{yzz} + 4/7\ \beta^2_{xyz} \quad (56)$$

Contribution from this term would reflect the out-of-plane twisting of the phenyl rings in the CV molecules. In the following, we will assume a D_{3h} symmetry for CV: the phenyl blades of the CV propeller configuration in solution experience a partially hindered rotation with respect to an equatorial plane around the three C^+-phenyl torsional axis leading to an average coplanar configuration, at the laser pulse time scale, hence our assumption of an averaged D_{3h} symmetry.

For C_{2v} and T_d planar molecules, the following expressions are obtained from Table 4:

$$\langle\beta_{C_{2v}}{}^2\rangle = 6/35\ \beta^2_{yyy} + 38/105\ \beta^2_{yxx} + 16/105\ \beta_{yyy}\beta_{yxx} \quad (57)$$

$$\langle\beta^2_{T_d}\rangle = 4/7\ \beta^2_{xyz} \quad (58)$$

The expressions have been obtained independently from ref 55, with more detailed calculation reported in Appendix E. Our agreement with the results in ref 55 points out some discrepancies with ref 56 which may contain partially erroneous results.

E. Experimental Results

1. Solvent Calibration

In the present context, solvents currently for their high dissolving power (acetone, chloroform, ethanol) must be calibrated with respect to a reference solvent already measured by the HLS technique. A reference β value also measured by way of HLS is more adequate than one chosen among molecules measured by the different EFISH techniques, where additional contributions from the electronic third-order hyperpolarizability γ_e may be present. We have therefore calibrated acetone and chloroform with respect to CCl_4, a solvent itself previously calibrated in ref 30 with respect to quartz, using the same HLS technique. Mixtures of CCl_4 and of the unknown solvent at various volumetric ratios have been tested. For acetone, we find $\langle\beta^2_{acet}\rangle/\langle\beta_{CCl_4}{}^2\rangle = 2.7$ and for chloroform, $\langle\beta_{CHCl_3}{}^2\rangle/\langle\beta_{CCl_4}{}^2\rangle = 1.36$. This ratio will be used, in the following, for $\langle\beta^2\rangle$ measurements of octopolar molecules in acetone. $\langle\beta^2\rangle$ can be determined with respect to $\langle\beta_{CCl_4}{}^2\rangle$ and therefore with respect to β_{xyz} of CCl_4, which was measured by the HLS technique by Terhune et al.[30]

Since ruthenium complexes are more soluble in ethanol, this solvent was used for β measurements, after a preliminary calibration with respect to the CCl_4 reference solvent; the $(\langle\beta^2\rangle)^{1/2}$ value was found to be similar to that of CCl_4 ($\langle\beta^2_{ethanol}\rangle^{1/2} = 0.28 \times 10^{-30}$ esu). It must be pointed out that only the knowledge of $(\langle\beta^2\rangle)^{1/2}$ values for reference solvents is required.

2. Measurement of the Crystal Violet Molecule

The following measurement procedure has been applied for crystal violet. CV is dissolved in acetone, whereas acetone has been previously referenced to CCl_4. The following expressions are then used:

$$\frac{\langle\beta^2_{CV}\rangle}{\langle\beta^2_{CCl_4}\rangle} = \frac{\langle\beta^2_{CV}\rangle}{\langle\beta^2_{acet}\rangle} \times \frac{\langle\beta^2_{acet}\rangle}{\langle\beta^2_{CCl_4}\rangle} \quad (59)$$

$$\langle\beta^2_{CCl_4}\rangle = 4/7\ (\beta^{CCl_4}_{xyz})^2 \quad (60)$$

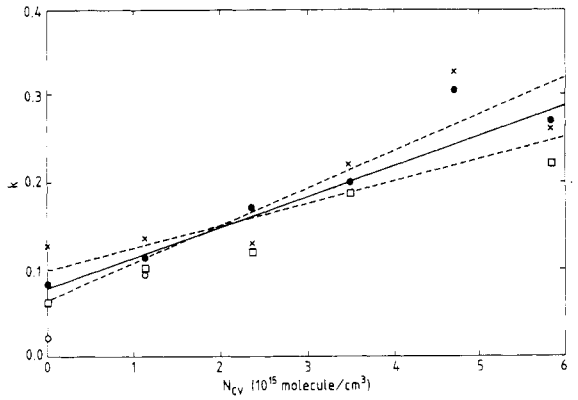

Figure 15. Plot of the experimental k values as a function of the number of CV molecules per volume unit. For each concentration, three measurements, corresponding respectively to ●, ×, and □, have been performed. The full line corresponds to the mean least-squares fit with the experimental linear behavior; the dotted lines are the minimal and maximal least-squares fits compatible with experimental data, providing an estimate of the experimental error.

as from T_d symmetry

$$\langle\beta^2_{CV}\rangle = 8/21\ (\beta^{CV}_{yyy})^2 \tag{61}$$

assuming a D_{3h} symmetry (see Table 4). Combination of these expressions leads to

$$\beta^{CV}_{yyy} = (3/2)^{1/2}\beta^{CCl_4}_{xyz}\left(\frac{I^{2\omega}_{CV}I^{2\omega}_{acet}}{I^{2\omega}_{acet}I^{2\omega}_{CCl_4}}\right)^{1/2}\left(\frac{N_{CCl_4}}{N_{CV}}\right)^{1/2} \tag{62}$$

While acetone has been previously referenced to CCl_4, the measurement of HLS from CV solutions is now detailed. Corrections originating from linear absorption at the harmonic frequency are taken into account in the data analysis, according to eq 53.

In the present configuration, the incident fundamental beam is vertically polarized; polarization effects were not evidenced on the harmonic wave, the depolarization factors introduced by the mirror and by the various other optical elements probably being dominant. Another possible reason for depolarization may originate from the contribution of presently neglected pseudotensorial ($J = 0$ and $J = 2$) irreducible β components. Presently undertaken frequency-dispersed HLS measurements will adress this issue. The $\langle\beta^2\rangle$ value measured by HLS is then the sum of the two terms $\langle\beta^2_{ZZZ}\rangle$ and $\langle\beta^2_{XZZ}\rangle$, where X is the propagation direction of the incident beam, Z the polarization direction of the fundamental incident wave, and Y the mean direction of observation of the scattered harmonic light. Adequate geometrical factors corresponding to each of these polarization components have been taken into account in the interpretation of experimental results.

The dependence of the k coefficient as a function of the concentration N_{CV} of the crystal violet molecule in acetone in plotted in Figure 15. For each concentration, several experimental points corresponding to different measurements performed on the same solutions, but in slightly different experimental conditions (maximal fundamental intensity, for example), are indicated. A least-squares fit analysis of these points gives a correlation factor higher than 0.9, corresponding to an overall relative error of the order of 25% and leading to

$$|\beta^{CV}_{yyy}| = 580 \times 10^{-30}\ \text{esu}$$

assuming a D_{3h} symmetry for CV.

The large value of the quadratic hyperpolarizability of crystal violet reflects the beneficial role of conjugation, of charge transfer, and possibly also of the ionic nature of CV. In addition to these structural features, resonance enhancement is partly responsible for the higher β value measured, as evidenced by the absorption spectrum in Figure 12. Taking a E_{01} value of 2.14 eV (λ_{max} = 590 nm) in eq 44, application of this equation to the CV molecule β tensor leads to a static $|\beta|$ value of 92 × 10^{-30} esu. This value is quite large compared to p-nitroaniline-like molecules.

Furthermore, one may want to question the validity of the D_{3h} molecular symmetry assumption, owing to possible out-of-plane rotations of the phenyl rings, reducing the molecular symmetry to that of a D_3 propeller.

Consideration of Table 3 shows that in such case, z-containing β coefficients will, strictly speaking, contribute to the measured signal. The β_{yyy} value must then be replaced by

$$\beta_{yyy}\left(1 + \frac{19}{10}\frac{\beta_{yzz}}{\beta_{yyy}} + \frac{3}{2}\frac{\beta_{xyz}}{\beta_{yyy}}\right)^{1/2}$$

It is however believed that z-containing β coefficients are small as compared to in-plane β_{yyy} and β_{yxx} ($= -\beta_{yyy}$) coefficients: quantum calculations should provide further insights into this issue.

3. Ruthenium Complexes

The same measurement technique, performed in ethanol, leads, for ruthenium complexes, to

$$(\langle\beta^2_{RuTB}\rangle/\langle\beta^2_{ethanol}\rangle)^{1/2} = 800 \pm 200 \text{ and } (\langle\beta^2_{RuTP}\rangle/\langle\beta^2_{ethanol}\rangle)^{1/2} = 600 \pm 150$$

and then

$$(\langle\beta^2_{RuTB}\rangle)^{1/2} = (230 \pm 60) \times 10^{-30}\ \text{esu and } (\langle\beta^2_{RuTP}\rangle)^{1/2} = (170 \pm 40) \times 10^{-30}\ \text{esu}$$

It is not possible, at this stage, to deduce from these averaged values the β_{yyy}, β_{yzz}, and β_{xyz} coefficients involved in the $\langle\beta^2\rangle$ value of molecules displaying a D_3 symmetry. The large value of the quadratic hyperpolarizability of ruthenium complexes reflects the beneficial role of MLCT charge transfer. As for CV molecule, it is however possible to deduce an estimate of the static hyperpolarizability using the dispersion relation of eq 44. Taking a E_{01} value of 2.76 eV (λ_{max} = 449 nm) leads to a static $|\beta|$ value of 53 × 10^{-30} esu for RuTB. For RuTP (λ_{max} = 434 nm), the static $|\beta|$ value is 47 × 10^{-30} esu, a value coming quite close to that of RuTB. These values are 5 times larger to that of p-nitroaniline-like molecules, and confirm the role of MLCT processes in the exaltation of β value by metal complexation.

F. Perspectives: HLS and EFISH Techniques

Whereas the initial experimental seed of this proposition had been the observation of a strong second-harmonic signal from a crystalline powder sample of

TATB,[5] the need for an adequate experimental scheme capable of screening molecular candidates at the solution level had been urgently felt since then. HLS is shown to provide an adequate experimental tool, to investigate the nonlinear properties of octopolar molecular or ionic solutions, which opens up in many ways the somewhat restricted access to β provided by the more traditional EFISH experiment. In the case of purely octopolar species, thus deprived of dipole moment, the EFISH experiment based on coherent second-harmonic generation from a collectively oriented assembly of molecular anharmonic oscillators, had been ruled-out from the start, hence the initial motivation of this work and the subsequent demonstration of the relevance of HLS in this context. Furthermore, some intrinsic limitations of the EFISH technique, even in cases where molecular orientation is achievable, can be supplemented by complementary HLS experiments. The EFISH signal[40] will provide access to the projection of the dipolar component of β on the ground-state dipole moment, namely:

$$\mu\,\beta = \mu\beta_{J=1}\cos\theta = \sum_{i,j}\mu_i\beta_{ijj} \qquad (63)$$

The summation on the right-hand side is performed over the Cartesian indices in the molecular reference frame, while the two expressions on the left are based on the rotationally invariant formalism. While the dipole moment μ is experimentally accessible by adequate measurements techniques performed in the same solvent environment as the EFISH experiment, the angle θ between the dipole moment and the dipolar β component has remained somewhat more elusive: one generally resorts to assumptions such as the parallelism between the two vectors (i.e. $\theta = 0$) in the case of quasi-1-D conjugated charge-transfer systems. This assumption is however highly questionable, as recently proved by theoretical quantum calculations performed on dipolar benzodithia polyenals and dithiolene polyenals of various conjugated extensions[57] with θ spanning a whole range of values from quasialigned ($\theta = 0$) to quasiperpendicular configurations ($\theta = 90°$). In the absence of additional information, a weak EFISH signal may thus be ascribed either to a small $\beta_{J=1}$ component, or to a quasiperpendicular configuration, or to both. Furthermore, the octopolar component $\beta_{J=3}$ is not accessible via an EFISH measurement with planar electrodes to pole the solution. It is thus worthwhile, in the case of a molecule of arbitrary symmetry entailing the presence of both $\beta_{J=1}$ and $\beta_{J=3}$ components, to perform both EFISH and HLS experiments. Let us illustrate the complementarity between the two approaches in the fairly general case of a planar molecule with C_{2v} symmetry. The EFISH experiment will provide

$$(I^{2\omega}_{\mathrm{EFISH}}) \approx \mu_y(\beta_{yyy} + \beta_{yxx}) \qquad (64)$$

whereas the unpolarized HLS signal will lead, as from Table IV, to

$$I^{2\omega}_{\mathrm{HLS}} \approx 6/35\,\beta^2_{yyy} + 38/105\,\beta^2_{yxx} + 16/105\,\beta_{yyy}\beta_{yxx} \qquad (65)$$

The two unknown tensorial coefficients β_{yyy} and β_{yxx} allowing for polarized detection along **X** and **Z** of the HLS signal, leading respectively to $I^{2\omega}_{\mathrm{HLS},X}$ and $I^{2\omega}_{\mathrm{HLS},Y}$, should directly provide the ratio $u = \beta_{yxx}/\beta_{yyy}$. As detailed in refs 2 and 3, this important parameter u reflects the in-plane anisotropy of the molecular nonlinear mechanism and is related to the ratio $\rho = \beta_{J=3}/\beta_{J=1}$ by

$$\rho = \beta_{J=3}/\beta_{J=1} = \frac{1}{\sqrt{3}}\,\frac{1-3u}{1+u} \qquad (66)$$

The depolarization ratio, obtained from Table 4, may be related to u and hence ρ by

$$\frac{I^{2\omega}_{\mathrm{HLS},X}}{I^{2\omega}_{\mathrm{HLS},Z}} = \frac{3\beta^2_{yyy} + 11\beta^2_{yxx} - 2\beta_{yyy}\beta_{yxx}}{15\beta^2_{yyy} + 27\beta^2_{yxx} + 18\beta_{yyy}\beta_{yxx}} = \frac{3 + 11u^2 - 2u}{15 + 27u^2 + 18u} \qquad (67)$$

The parameter u has been shown to be amenable to molecular engineering considerations,[2] whereas the simplified 1-D model forces u to cancel ($u = 0$ and $\rho = 1/\sqrt{3}$). Adequate molecular design schemes, such as proposed in ref 20, allow one to span a considerable range of u values with worthwhile experimental implications linked to the availability, at the macroscopic level, of two or more β tensor coefficients.

The new and so far experimentally elusive class of octopolar nonlinear molecules and ions has been shown to be amenable to solution investigations, via HLS experiments, with crystal violet and Ruthenium complexes, providing the first evidence of a strong nonlinear response from a trigonal charge transfer conjugated cation. Additional frequency-dispersed HLS measurements with a tunable infrared source, presently under way, should help sort out questions pertaining to the spectroscopy of octopolar molecules and the related issue of β resonant enhancement and depolarization factor.

Furthermore, the HLS experiment should be applied to revisit the more traditional dipolar systems, so as to complement a purely dipolar β information, as from EFISH, by otherwise unaccessible β coefficients. Such enriched experimental feedback should encourage chemists to explore the possibilities of fully three-dimensional synthetic pathways, in keeping with the so far poorly exploited anisotropic nature of molecular hyperpolarizability tensors. While more efficient nonlinear molecules and materials are prone to emerge from such combined renewal of experimental methods and molecular engineering schemes, one may also expect a better insight onto the nature of charge-transfer mechanisms in complex polysubstituted 3-D molecular systems.

VI. Macroscopic Ordering and Optical Interactions

While packing of 1-D nonlinear molecules has been thoroughly investigated, with best orientations for phase-matched processes and a corresponding "magic angle" evidenced,[19] the situation is more complex for truly planar systems such as octopoles. We shall first consider some simple specific cases in the realm of single crystals to help illustrate the present point of view.

The lamellar 2-D octopolar macroscopic ordering of TATB can be ascribed to "heteroaffinity" between side groups of different origins:[5] a H-bonding network locks the nitro group of a given molecule to the amino group

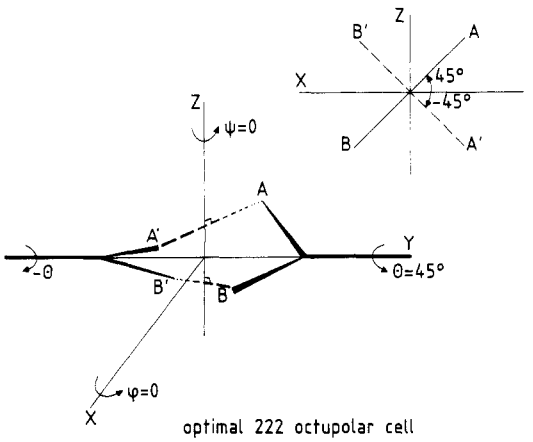

Figure 16. Optimization of molecular orientations for planar octopoles and the 222 crystal point group. The most favorable orientation for quadratic nonlinear optics when θ is varied is obtained at $\theta = \pi/4$.

of one of its six neighbors, thus inducing optimal trigonal arrangement. Conversely, homoaffinity would be prone to induce a detrimental centrosymmetric hexagonal packing. The metaborate mineral ionic crystal (BBO) exemplifies a staggered columnar octopolar packing of cyclic $(B_3O_6)^{3-}$ anionic octopoles.[58,59] The nonlinearity in L-argininium phosphate (LAP)[60] and its deuterated form dLAP[61] crystals can be at least partially ascribed to a quasitrigonal guanidinium-like fragment in a chiral structure. Cocrystallization of guanidinium with tartaric acid has been recently considered[43] and shown to lead to a noncentrosymmetric, however not optimal, crystalline structure: its 222 orthorhombic structure is composed of strongly interlocked strands of aggregated monohydrogen L-tartrate polyanion chains hosting guanidinium ions at their intersections. Its SHG powder efficiency compares to that of urea and could be improved by 1 order of magnitude at least[43] by increasing the angle between corresponding octopole guanidinium planes from an actual 16° to the optimal 90° as shown in Figure 16.

Simple considerations, pertaining to statistical averaging in eq 24 or mere inspection of the character tables of the Abelian planar rotation group, evidence that the relevant order parameters for lamellar or planar *statistical* octopolar ordering are $\langle\cos 3\theta\rangle$ and $\langle\sin 3\theta\rangle$ defined as averaged values over the statistical distribution of molecular orientation angles away from a fixed laboratory framework parallel to the octopolar planes. In the case of crystalline structures, the averaging has to be replaced by a finite summation over molecular sites in the unit cell divided by the number of sites.

A macroscopic assembly of octopoles may be either the result of self-assembly and hence reflect an intricate mixture of shape, affinity, and charge-related features making up for a crystalline structure or a mesophase, or it may alternatively be obtained from an adaptation of the well-known poling procedure traditionally used in the context of amorphous polymers embedding dipolar nonlinear moieties. However, the classical poling procedure[62] will not operate for octopoles in the absence of dipole moment. A possible solution, at least in principle, is to resort to a "multipoling" procedure[1] by way of extension of the classical poling technique, where a symmetry-adapted multipolar field distribution is generated in an adequately electroded cell. Such a multipolar potential will couple to a multipolar charge distribution of same multipolar order and ensure the poling energy. In other words, the J component of a multipoling potential tensor (i.e. the spatial derivative of the potential at the required order $\partial^{(n)}V/\partial x_1...\partial x_n$) will only couple to the component of same irreducible order J of the multipolar charge distribution. However the magnitude of the multipoling coupling term is expected to decrease exponentially with the multipolar order n, following a r^n/R^{n+1} law where r scales with the molecular dimension and R with that of the electroded cell while n refers to the 2^n order of the multipole. Multipoling could then be ideally achieved in guest–host "supramolecular" compounds whereby the multipoling host size is scaled down to the molecular scale (i.e. $r \approx R$). Octopoling, for example, could then be ensured by hosting a trigonal nonlinear microscopic molecule in an octopoling trigonal or tetrahedral lattice. One may then envision octopolar guest–host supramolecular systems, a first example of which being the previously mentioned guanidinium tartrate lattice[43] where the tartrate anion should be traded for a more adequate octopolar hosting structure.

A different approach, based on an all-optical poling by means of a six-wave mixing time-resolved phase-conjugation geometry initially applied to dipolar molecules in solution,[63] has been recently extended to octopolar molecules.[64] This configuration is based on the nonzero time-averaged values of $\langle(E_\omega+E_{2\omega})^3\rangle$ where the material is simultaneously shined by ω and 2ω radiation. A formally similar mechanism had been invoked to account for second-harmonic generation in glass fibers.[65,66] The excited-state lifetime of ethyl violet in a viscous solution of propane-1,2-diol has been found to be of the order of 26 ps in a pump–probe configuration. Furthermore, variation of ω and 2ω polarizations has permitted one to probe and validate the postulated octopolar symmetry of the underlying β tensor of ethyl violet. Moreover, permanent poling of ethyl violet in a sol–gel film has been demonstrated along the lines developed in ref 65: it is possible to imprint a quasi-phase-matched grating with inverted $\chi^{(2)}$ domains scaling with the coherence length $2\pi(k_{2\omega}-k_\omega)^{-1}$ after seeding with ω and 2ω beams.[67] The photochemistry involved, clearly related to *cis–trans* photoisomerization in the case of DANS-like chromophores, is still to be unveiled and further optimized for triphenylmethanes as well as other potentially interesting species.

Besides their interesting conformational and packing structural properties to be revealed by X-ray diffraction, macroscopic nonlinear octopolar assemblies may possess remarkable nonlinear optical properties, especially in what pertains to optical polarization behavior.

Irreducible tensorial decomposition has been so far consistently applied both to nonlinear optical susceptibilities and also, however to a lesser extent in section III, to the field tensor defined in eq 41 (or eq 42) for quadratic (cubic) nonlinear interactions. In the case of second-harmonic generation, the averaged energy transferred via the nonlinear medium per unit time from the fundamental to the harmonic wave is proportional to $(\boldsymbol{E}^{2\omega})^* \, \mathrm{d}\boldsymbol{P}_{NL}^{2\omega}/\mathrm{d}t$ where $(\boldsymbol{E}^{2\omega})^*$ (or $\boldsymbol{P}_{\mathrm{NL}}^{2\omega}$) is the harmonic field (harmonic-induced polarization).[68] Finally the averaged harmonic energy conversion rate is

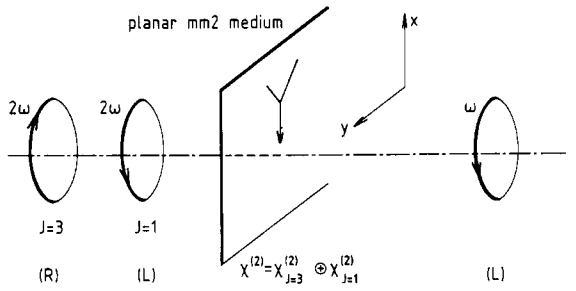

Figure 17. Right-handed (or left-handed) circularly polarized fundamental laser light impinging on a planar molecular array may be up-converted by collinear SHG at normal incidence in the sum of a left-handed (right-handed) circularly polarized harmonic beam originating from the octopolar component of the nonlinearity and of a right-handed (left-handed) circularly polarized harmonic beam originating from the dipolar component. The medium is assumed to be two-dimensional with X as a 2-fold in-plane symmetry axis. Due to birefringence, elliptization of the circular polarizations, not represented here, may modify the analysis and should also be taken into account.

given by

$$dW/dt \propto -\sum_{J=1,3} \chi_J^{(2)} \langle F_J^{(2)} \rangle \tag{68}$$

In this expression, summation is performed over tensorial contractions of the irreducible components of identical weight J of $\chi^{(2)}$ and of the field tensor $F^{(2)}$ as previously defined in section III (the brackets refer to time averaging over one period at 2ω). Cross terms between $J = 1$ and $J = 3$ components are ruled-out by orthogonality of irreducible subspaces.

It is of particular interest in the present context to identify the nature of the $J = 1$ and $J = 3$ components of the $F^{(2)}$ field tensor in terms of the polarization modes of the interacting fields, so as to match the corresponding components of the $\chi^{(2)}$ susceptibility tensor. In the subsequent analysis, we concentrate, for the sake of simplicity, on a simple configuration depicted in Figure 17: a 2-D lamellar nonlinear medium with molecular as well as crystalline planes parallel to the $(\boldsymbol{X},\boldsymbol{Y})$ framework is shined at normal incidence by a fundamental beam at frequency ω. It is further assumed that the $\boldsymbol{X}$ axis is a 2-fold crystalline symmetry axis, any rank-3 symmetrical tensor attached to the medium being then of dimension two with only XXX and XYY labeled components. Note that a planar 2-D octopolar medium, such as a crystalline plane of TATB parallel to the molecular planes, is a special case of this configuration with tensorial dimension reduced to one. The $J = 1$ and $J = 3$ irreducible spaces are both 1-D and respectively spanned by the normalized tensors $^3/_4\boldsymbol{X} \otimes (\boldsymbol{X} \otimes \boldsymbol{X} + \boldsymbol{Y} \otimes \boldsymbol{Y})$ and $^1/_4\boldsymbol{X} \otimes (\boldsymbol{X} \otimes \boldsymbol{X} - 3\boldsymbol{Y} \otimes \boldsymbol{Y})$. Identification of the ω and 2ω polarizations leading to $J = 1$ and $J = 3$ irreducible components of $F^{(2)}$ is then straightforward. The $J = 1$ component corresponds to circularly polarized ω and 2ω polarizations with same left-handed or right-handed orientations. Taking $\mathbf{E}^{\omega,2\omega} = E^{\omega,2\omega}(\boldsymbol{X} + \epsilon j \boldsymbol{Y})$ leads to

$$F^{(2)} = E^{2\omega}(E^{\omega})^2 \boldsymbol{X} \otimes (\boldsymbol{X} \otimes \boldsymbol{X} + \boldsymbol{Y} \otimes \boldsymbol{Y}) = F^{(2)}_{J=1} \tag{69}$$

where $\epsilon = \pm 1$ depends on the orientation of the circular polarization. It is crucial in this calculation and following ones to retain the complex conjugated expression (i.e. starred notation in eqs 41 and 42) of the harmonic field. Conversely, taking ω and 2ω beams as inversely circularly polarized beams (e.g. ω right-handed and 2ω left-handed or vice versa) leads to

$$F^{(2)} = E^{2\omega}(E^{\omega})^2 \boldsymbol{X} \otimes (\boldsymbol{X} \otimes \boldsymbol{X} - 3\boldsymbol{Y} \otimes \boldsymbol{Y}) = F^{(2)}_{J=3} \tag{70}$$

with

$$\mathbf{E}^{\omega} = E^{\omega}(\boldsymbol{X} + \epsilon j \boldsymbol{Y}) \tag{71}$$

$$\mathbf{E}^{2\omega} = E^{2\omega}(\boldsymbol{X} - \epsilon j \boldsymbol{Y}) \tag{72}$$

Assuming a purely $J = 1$ (or $J = 3$) 2-D medium with $mm2$ symmetry as shown in Figure 17, the relevant ω and 2ω polarization combination will be precisely that leading to the same purely $J = 1$ ($J = 3$) $F^{(2)}$ tensor. In the case of a purely $J = 1$ polar medium, right-handed circularly polarized light will be converted into right-handed circularly polarized light (similarly for left-handed circularly polarized light). Hence the right- or left-handed nature of a circularly polarized beam is left unchanged in the upconversion process. Conversely, SHG in a purely $J = 3$ octopolar medium will reverse the orientation of incoming circularly polarized light into inversely circularly polarized harmonic light. In a more general medium, such as depicted in Figure 17 and defined above, right-handed circularly polarized fundamental light will give rise to the sum of right-handed circularly polarized harmonic light, in response to $\chi^{(2)}_{J=1}$ and left-handed circularly polarized harmonic light, as from $\chi^{(2)}_{J=3}$. Left and right can of course be permuted in this statement. In practice, elliptization due to the birefringence of the medium will also take place, depending on the thickness of the sample: the analysis developed here must then be accordingly modified but will still retain the basic properties outlined here, such as the possible reversal of circular polarization reflecting the prevailing magnitude of the octopolar β component over that of the dipolar one.

VII. Conclusion

An original type of molecular and material structures for quadratic nonlinear optics, which may be less hampered by drawbacks linked to more traditional designs, has been described and further shown to manifest specific advantages of its own. The definition of such structure results from a deliberate attempt to optimize the octopolar part of β and $\chi^{(2)}$ while strictly canceling their vectorial components. The main detrimental features associated to dipolar structures may now be faced with more favorable assets in view of the specific features of octopolar structures:

—The more rounded-off shape of octopolar molecules should ease their packing in a single crystalline lattice as opposed to less favorable elongated dipolar sometimes rodlike molecules.

—The absence of dipolar moments should improve the statistics for favorable noncentrosymmetric structures as had been initially argued, however in a less systematic way, for POM crystals.[9]

—A trigonal lamellar structure ensures $r_{13} = -r_{33}$ which should allow one to increase the capacity of electrooptic modulators: as shown on Figure 18, equally efficient modulation of TE and TM modes is then possible, contrary to traditional dipolar structures used

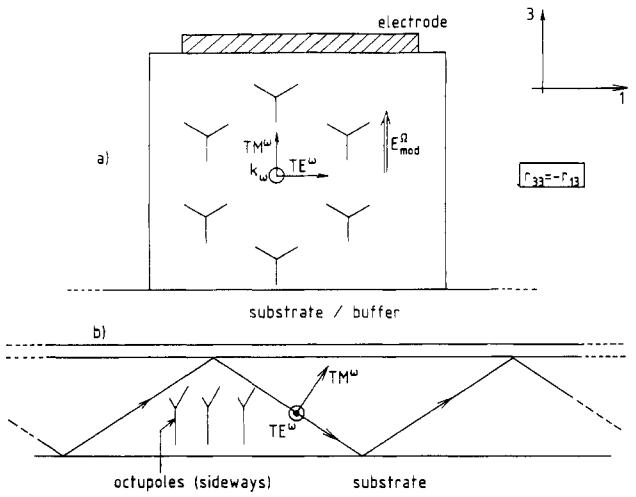

Figure 18. Simplified views of an *octopolar* electrooptic channel waveguide where octopolar nonlinear chromophores are aligned. Crystalline alignment or statistical *octopoling* ensure that $r_{33} = r_{13}$: TE as well as TM modes can then be modulated with similar efficiencies especially for low order modes. Part a is a transverse section perpendicular to the propagation direction. Part b is a sideways view parallel to the propagation axis.

in poled polymers, which favor r_{33} over r_{13} and hence apply only to a unique polarization mode along 3.

—The tendency toward aggregation, as for polar dyes, should be strongly influenced by the absence of dipole, and in some cases decreased.

—The transparency as well as efficiency of adequately tailored octopolar molecules are expected in different instances to significantly improve over that of their dipolar counterparts.[8]

Finally, on the basis of recent experimental results,[64,67] the possibility to permanently pole octopolar nonlinear chromophores in an all-optical configuration opens up new challenging perspectives.

Development of a new, fairly general family of both molecules and materials is now being undertaken following the molecular engineering guidelines proposed here. Harmonic light scattering should consistently provide the relevant experimental scheme toward the determination of octopolar β's. Whereas current research strategies may have narrowed the synthetic exploration domain to simpler quasi-1-D molecular systems, more advanced molecular engineering guidelines aiming at the tailoring of an adequately balanced combination of irreducible tensorial components of nonlinear susceptibilities are to be developed: such an approach has been exemplified here in the case of octopolar nonlinear systems, consistently so at both molecular and macroscopic levels. Further work currently under way and expanding over the concepts exposed here should permit one to fully benefit, within the context of nonlinear optics, from the hitherto poorly exploited 3-D nature of organic systems.

Acknowledgments. We are grateful to Professor Robert Silbey, Drs. Dave Yaron and Manuel Joffre from the Department of Chemistry at MIT for a fruitful collaboration in the quantum chemistry part of this work and to Christophe Dhenault and Thai Chauvan for their help in the experimental part.

Appendix A. Introduction to Irreducible Representation of Tensors

We will attempt in the following to provide a brief and intuitive introduction to irreducible tensor representation, starting from well-known results in Fourier theory and spherical harmonic analysis. The following considerations cannot be a substitute for the more thorough and technical developments found, for example, in refs 11 and 15, the aim being here to supply an introduction to the essential concepts that will be needed hereafter.

We start by considering a scalar function of the polar angle θ with corresponding 2π periodicity. Such a function may be expanded in Fourier series according to

$$f(\theta) = \sum_{J=-\infty}^{+\infty} f_J(\theta) = \sum_{J=-\infty}^{+\infty} f_J e^{jJ\theta} \tag{A1}$$

with

$$f_J = 1/2\pi \int_0^{2\pi} f(\theta) e^{-jJ\theta} d\theta \tag{A2}$$

Rotation of the function f by an angle θ_0 (operator R below) is then readily performed in the Fourier representation by

$$R[f] = f(\theta - \theta_0) = \sum_{J=-\infty}^{\infty} f'_J e^{jJ\theta} \tag{A3}$$

with

$$f'_J = e^{jJ\theta_0} f_J \tag{A4}$$

Functions $f_J(\theta_0)$ can be viewed as irreducible representations of f with respect to the group of in-plane rotations. Irreducible subspaces are one-dimensional as a consequence of the commutative nature of this group and the phase term in eq A4 is simply the character of the corresponding representation.

By way of extension, a function $F(\theta,\phi)$ defined over spherical angle coordinates can be expanded in terms of spherical harmonics $Y_m^J(\theta,\phi)$ following

$$F(\theta,\phi) = \sum_{J=0}^{\infty} F_J(\theta,\phi) = \sum_{J=0}^{\infty} \sum_{m=-J}^{m=J} F_{J,m} Y_m^J(\theta,\phi) \tag{A5}$$

with the $F_{J,m}$'s given by

$$F(\theta,\phi) = \int_0^{2\pi} d\phi \int_0^{\pi} d\theta\, F(\theta,\phi) Y_m^{J*} \sin\theta \tag{A6}$$

The F_j's are irreducible components of F expressed in irreducible functional spaces of weight J and dimension $2J + 1$ spanned by the Y_m^J's ($-m \leq J \leq m$).

Very much like in 2-D space, 3-D rotations (defined by the Euler angles θ, ϕ, and ψ and the operator R), can be readily performed in irreducible functional spaces by application of the Wigner matrix elements accounting for the rotation of spherical harmonics, namely:

$$R(\theta,\phi,\psi)[Y_m^J] = \sum_{m'=-J}^{J} D_{m,m'}^J Y_{m'}^J \tag{A7}$$

Application of eq A7 to eq A6 leads, after reordering of terms in the summation, to

$$F_{J,m'} = \sum_{m'=-J}^{J} D^{J}_{m,m'} F^{J}_{m'} \quad \text{(A8)}$$

where the $F_{J,m'}$'s are the coefficients of the development of the rotated function over spherical harmonics.

Alternatively, 2-D and 3-D functions f and F can be respectively defined over the unit circle and the unit sphere by use of Cartesian variables, namely:

$$f = f(\theta) = f(x = \cos\theta, y = \sin\theta) \quad \text{(A9)}$$

and

$$F = F(\theta,\phi) = F(x = \sin\theta\cos\phi, y = \sin\theta\sin\phi, z = \cos\theta) \quad \text{(A10)}$$

Handling of rotations in Cartesian representation of functions can be very tedious as opposed to the previous simple and "universal" expressions A3, A4, and A7.

Let us now consider tensors of arbitrary rank n which will be assumed, for the sake of simplicity, to be symmetric with respect to the permutation of their Cartesian indices. There is a one-to-one correspondence between symmetric tensors of rank n, $\mathbf{T}^{(n)}$, and homogeneous polynomials of degree n, thus allowing to use the following notation:

$$T^{(n)} = T^{(n)}(\theta,\phi) = T^{(n)}_{i_1,i_2\ldots i_n}\mathbf{x}_{i_1}\mathbf{x}_{i_2}\ldots\mathbf{x}_{i_n} \quad \text{(A11)}$$

with i_j labeling one of the three coordinate directions. One may then take $T^{(n)}$ as a function of the sole angular parameters θ and ϕ, as it is sufficient to define a homogeneous function over the unit sphere. This one-to-one correspondence then permits to consider a symmetrical tensor $T^{(n)}$ of rank n as a homogeneous polynomial of rank n defined over the unit sphere. It is then possible to apply expressions A5 and A6 to $\mathbf{T}^{(n)}$ with an essential simplification brought about by the polynomial nature of $T^{(n)}$ in terms of cosine and sine trigonometric functions of θ and ϕ. It can be easily proved that the infinite summation in eq A5 can be truncated for $J > n$, hence

$$T^{(n)} = \sum_{J=0}^{n} T^{(n)}_{J} = \sum_{J=0}^{n}\sum_{m=-J}^{J} T^{(n)}_{J,m} \quad \text{(A12)}$$

with

$$T^{(n)}_{J,m} = t^{n}_{J,m} Y^{J}_{m} \quad \text{(A13)}$$

and

$$t^{(n)}_{J,m} = T_{i_1\ldots i_n}\int x_{i_1}\ldots x_{i_n} Y^{J*}_{m} \sin\theta\, d\theta\, d\phi \quad \text{(A14)}$$

Expression A14 outlines the correspondence between Cartesian and irreducible components which is fully developed in ref 15. For the more general case of nonsymmetrical Cartesian tensors (e.g. Kleinman nonvalid), one may refer to the algebra of noncommutative polynomials and straightforwardly generalize this presentation.

Appendix B. Multipolar Groups of Order L: Definition and Criteria

For the sake of clarity, we shall start from a rigorous, group theory based definition of polar groups (i.e. multipolar groups of order $L = 1$) and then proceed to generalize the definition and related criterion to higher multipolar orders.

The notion of polar group is frequently referred to when discussing symmetry operations which are compatible with observable properties depicted by a vector such as the dipole moment of molecules, the spontaneous polarization in ferroelectric materials, or the vectorial component to the quadratic hyperpolarizability β, the latter being of relevance in the interpretation of solution EFISH experiments or poled electrooptic polymers. It is possible to establish a rigorous criterion, on the basis of irreducible group representation theory, so as to discriminate between polar and nonpolar groups as follows: the irreducible representations of the 3-D rotation group SO_3, labeled D_L following Wigner,[11] have dimension $2L + 1$ and may eventually be further reduced with respect to a subgroup G of SO_3 which is assumed to keep the molecule or material invariant. When the representation space is that of complex functions defined on the unit sphere, a well-known convenient basis set for D_L is made-up of the $2L + 1$ spherical harmonics of order L, namely $Y^{m}_{L}(\theta,\phi)$.

Starting with $L = 1$, the D_1 space becomes reducible when serving as a representation space for G and may then be expanded into a direct sum of vector subspaces adequately chosen among the irreducible representations of group G. This new decomposition of D_1 may or may not contain A_1, the 1-D totally symmetrical irreducible representation of G with characters all set equal to 1. In the former case, the group is compatible with the existence of invariant vectorial quantities and is said to be polar.

This approach can then be naturally generalized as follows: suppose that all representations D_l, with $1 < l < L$, when decomposed in irreducible representations of the subgroup G, are deprived of the fully symmetrical representation A_1, while D_L stands out as the lowest order representation which contains the A_1 representation at least once. This property will then serve as the definition of a multipolar group of order L. Of course, the special case $L = 0$ has been ruled out as the $D_{L=0}$ space strictly coincides with A_1, another way of stating that scalar quantities (i.e. charge or pressure, for example) are invariant with respect to rotations. In more physical terms, this statement relates to the obvious impossibility of fully canceling the polarizability tensor of a molecule ($\alpha_{J=0}$ or the trace of α can indeed never be zero) as well as that of lowering the index of refraction of matter below one. This definition obviously encompasses that of polar groups which correspond to the special case $L = 1$.

The a priori unknown multipolar order of a group can be straightforwardly determined from simple manipulation of group character tables, following the previously proposed definition. Calling Γ_i the irreducible representations of the subgroup G of SO_3 and a^{L}_{i} the number of occurences of Γ_i in D_L, the following decomposition can be obtained:

$$D_L = \bigotimes_i a^{L}_{i}\Gamma_i \quad \text{(B1)}$$

$$a^{L}_{i} = h^{-1}\sum_{k} N_k \chi_i(C_k)\chi_L(C_k) \quad \text{(B2)}$$

where h stands for the number elements (e.g. symmetry operations) of group G, the classes of G, labeled by k, are called C_k; $\chi_i(C_k)$ (or $\chi_L(C_k)$) is the character of the irreducible (reducible) representation Γ_i (D_L) for class C_k and N_k is the number of elements in C_k. We are interested here in $\Gamma_i = A_1$, the fully symmetrical representation, in which case all the $\chi_i(C_k)$'s are equal to 1 and the number of occurrences of A_1 in D_L, called a_i^L is given by

$$a_i^L = h^{-1}\sum_k N_k \chi_L(C_k) \tag{B3}$$

If C_k corresponds to rotations of angle α_k, $\chi_L(C_k)$ is given by

$$\chi_L(C_k) = \frac{\sin(L + {}^1/_2)\alpha_k}{\sin \alpha_k/2} \tag{B4}$$

We finally obtain the following operational criterion: the group G is multipolar of order L when $a_1^l = 0$ for $0 < l < L$ and $a_1^L > 0$.

Let us exemplify this definition in the two simple cases of the tetrahedral (T) and octahedral (O) groups. T is the simplest cubic group made up of the 12 proper rotational operations which keep a regular tetrahedron invariant. O is the group of 24 proper rotations which keep a cube or an octahedron invariant. Both are subgroups of SO_3. The relevant character tables for this analysis, readily found in any textbook on group representation theory, will help derive from eq B3 the following set of a_1^L values, up to $L = 4$: $a_1^0 = 1$, $a_1^1 = a_1^2 = 0$, $a_1^3 = 1$ for group T; and $a_1^0 = 1$, $a_1^2 = a_1^3 = 0$, $a_1^4 = 1$ for group O.

Following the proposed terminology, T may be called an octopolar group and O an hexadecapolar group.

The following general theorem can then be readily established: if a material system is invariant with respect to a multipolar group of order L, then all physical properties behaving like multipoles of order $1 < l < L$ will strictly vanish. In particular, if the group is quadrupolar, all vectorial quantities will vanish, if it is octopolar, dipolar and quadrupolar properties will cancel and so forth. As a consequence of this property, one may note that planar molecules invariant under 5-fold symmetry (e.g. eclipsed ferrocene) cannot sustain rank-3 tensorial properties such as a β hyperpolarizability. This property and generalizations are indeed amenable to intuition: the stronger the symmetry constraint, such as attached to higher order rotational symmetry, the more coefficients or combinations therefrom are forced to cancel in order to comply with symmetry invariance. Low-order tensors will then see all their coefficients cancel while higher order ones, although partially affected by symmetry constraints, will be able to sustain them without complete cancellation. In this appendix, a more rigorous formulation of this intuitive evidence has been proposed.

Appendix C. Irreducible Components of Rank-3 Symmetric Tensors in Cartesian Notation

The vector and octopolar Cartesian components of a symmetric rank-3 tensor, such as β or $\chi^{(2)}$ microscopic and macroscopic susceptibilities in the spectral range of validity of Kleinman symmetry relations, are being detailed hereafter in an orthonormal (e_X,e_Y,e_Z) framework. The dimension of the vector space of rank-3 symmetrical tensors is 10. We shall adopt in this appendix the following unambiguous notation so as to shorten expressions of tensors: X^3 (or X^2Y) will for example stand for the symmetric tensor product basis set elements $e_X \otimes e_X \otimes e_X$ ($e_X \otimes e_X \otimes e_Y$ or any of the equivalent two other permutations, sometimes noted with O instead of $\otimes$). In addition to its simplicity, this notation permits one to take straightforward advantage of the formal equivalence between symmetrical tensors in 3-D space and homogeneous polynomials of three variables: in particular, tensor products or multilinear forms acting on 3-D vectors will transform under symmetry operations exactly as homogeneous polynomials after adequate variable substitution. While that simple formal equivalence rule should suffice, in practice, in what follows, to the reader unfamiliar with tensor manipulation, detailed foundations can be found in ref 17. Within our conventions, the general Cartesian expression for tensor β corresponding to a 3-D object is

$$\begin{aligned}\beta = {} & \beta_{XXX}X^3 + \beta_{YYY}Y^3 + \beta_{ZZZ}Z^3 \\ & + 3\beta_{XYY}XY^2 + 3\beta_{YXX}YX^2 + 3\beta_{XZZ}XZ^2 + \\ & 3\beta_{ZXX}ZX^2 + 3\beta_{YZZ}YZ^2 + 3\beta_{ZYY}ZY^2 \\ & + 6\beta_{XYZ}XYZ\end{aligned} \tag{C1}$$

Note that coefficients 3 and 6 present throughout this expression and the following ones stand for symmetric tensorial products, for example $3XYY$ instead of $XYY + YXY + YYX$ and $6XYZ$ instead of the $3! = 6$ permutations of X, Y, and Z. This distinction becomes important when squaring individual β_{ijk} coefficients to yield β. The vector part of a general β tensor is given by

$$\begin{aligned}\beta_{J=1} = {} & 3/5\,[(\beta_{XXX} + \beta_{XYY} + \beta_{XZZ})X + (\beta_{YXX} + \\ & \beta_{YYY} + \beta_{YZZ})Y + (\beta_{ZXX} + \beta_{ZYY} + \beta_{ZZZ})Z](X^2 + \\ & Y^2 + Z^2)\end{aligned} \tag{C2}$$

The normalization factor $\lambda = {}^3/_5$ may be straightforwardly obtained from the condition that the vectorial contribution to the octopolar component of β identically vanishes, i.e.

$$[\beta_{J=3}]_{J=1} = [\beta - \lambda\beta_{J=1}]_{J=1} = 0 \tag{C3}$$

The dimension of the vectorial tensorial subspace is 3 in accordance with the dimension of the $J = 1$ ($m = +1, 0, -1$) subspace of spherical harmonics. The octopolar component is obtained by substracting to the general expression of β as in eq C1 the vectorial component as from eq C2:

$$\begin{aligned}5\beta_{J=3} = {} & [4\beta_{XYY} - (\beta_{XXX} + \beta_{XZZ})]X(3Y^2 - X^2) \\ & + [4\beta_{XZZ} - (\beta_{XXX} + \beta_{XYY})]X(3Z^2 - X^2) \\ & + [4\beta_{YXX} - (\beta_{YYY} + \beta_{YZZ})]Y(3X^2 - Y^2) \\ & + [4\beta_{YZZ} - (\beta_{YYY} + \beta_{YXX})]Y(3Z^2 - Y^2) \\ & + [4\beta_{ZXX} - (\beta_{ZZZ} + \beta_{ZYY})]Z(3X^2 - Z^2) \\ & + [4\beta_{ZYY} - (\beta_{ZZZ} + \beta_{ZXX})]X(3Y^2 - Z^2) \\ & + 30\beta_{XYZ}XYZ\end{aligned} \tag{C4}$$

As expected, the $J = 3$ octopolar subspace has dimension 7.

In the case of a symmetrical molecule, the corresponding β tensor will sustain less than 10 zero nonvanishing components so as to abide to specific symmetry constraints. The vectorial and octopolar components in eqs C2 and C4 will then take simpler forms to be detailed hereafter for point groups C_{2v}, $C_{\infty v}$, 222, C_3, C_{3v}, and D_{3h}.

C_{2v}. The 2-fold axis is along Z and the two mirror planes are (ZX) and (ZY). The general form for β is

$$\beta = \beta_{ZZZ}Z^3 + 3\beta_{ZXX}ZX^2 + 3\beta_{ZYY}ZY^2 \quad \text{(C5)}$$

$$5\beta_{J=3} = [4\beta_{ZYY} - (\beta_{ZZZ} + \beta_{ZXX})](3ZY^2 - Z^3) + [4\beta_{ZXX} - (\beta_{ZZZ} + \beta_{ZYY})](3ZX^2 - Z^3) \quad \text{(C6)}$$

$$\beta_{J=1} = 3/5\ (\beta_{ZZZ} + \beta_{ZXX} + \beta_{ZYY})Z(X^2 + Y^2 + Z^2) \quad \text{(C7)}$$

$C_{\infty v}$. The symmetry axis is along Z. A symmetric rank-3 tensor has only two independent components, namely $\beta_\parallel$ and $\beta_o = \beta_{ZXX} = \beta_{ZYY}$. The general form of a $C_{\infty v}$ tensor is then given by

$$\beta = \beta_\parallel Z^3 + 3\beta_o Z(X^2 + Y^2) \quad \text{(C8)}$$

$$5\beta_{J=3} = (3\beta_o - \beta_\parallel)Z(3X^2 + 3Y^2 - 2Z^2) \quad \text{(C9)}$$

$$\beta_{J=1} = 3/5\ (\beta_\parallel + 2\beta_o)Z(X^2 + Y^2 + Z^2) \quad \text{(C10)}$$

222. The three 2-fold axes are respectively along X, Y, and Z. The β tensor reduces to a purely octopolar component and its vector part is identically zero:

$$\beta = \beta_{J=3} = 6\beta_{XYZ}XYZ \quad \text{(C11)}$$

C_3. The 3-fold axis is along Z. The general form of a symmetric rank-3 tensor is

$$\beta = \beta_{ZZZ}Z^3 + 3\beta_{ZXX}Z(X^2 + Y^2) + \beta_{XXX}X(X^2 - 3Y^2) + \beta_{YYY}Y(Y^2 - 3X^2) \quad \text{(C12)}$$

The octopolar and vector parts are respectively given by

$$\beta_{J=3} = 1/5\ (\beta_{ZZZ} - 3\beta_{ZXX})Z(2Z^2 - 3Y^2 - 3X^2) + \beta_{XXX}X(X^2 - 3Y^2) + \beta_{YYY}Y(Y^2 - 3X^2) \quad \text{(C13)}$$

$$\beta_{J=1} = 3/5\ (\beta_{ZZZ} + 2\beta_{ZXX})Z(X^2 + Y^2 + Z^2) \quad \text{(C14)}$$

C_{3v}. The 3-fold axis is along Z. The general form of a symmetric rank-3 tensor is

$$\beta = \beta_{ZZZ}Z^3 + 3\beta_{ZXX}Z(X^2 + Y^2) + \beta_{XXX}X(X^2 - 3Y^2) + \beta_{YYY}Y(Y^2 - 3X^2) \quad \text{(C15)}$$

The octopolar and vector parts are respectively given by

$$\beta_{J=3} = 1/5\ (\beta_{ZZZ} - 3\beta_{ZXX})Z(2Z^2 - 3Y^2 - 3X^2) + \beta_{XXX}X(X^2 - 3Y^2) + \beta_{YYY}Y(Y^2 - 3X^2) \quad \text{(C16)}$$

$$\beta_{J=1} = 3/5\ (\beta_{ZZZ} + 2\beta_{ZXX})Z(X^2 + Y^2 + Z^2) \quad \text{(C17)}$$

D_{3h}. This group is obtained from the C_{3v} group by addition of a mirror plane perpendicular to the 3-fold axis which precludes nonzero coefficients with an odd number of Z indices and leads in particular to the cancellation of the vector part of β.

$$\beta = \beta_{J=3} = \beta_{XXX}X(X^2 - 3Y^2) + \beta_{YYY}Y(Y^2 - 3X^2) \quad \text{(C18)}$$

When the mirror plane containing the Z axis is (ZX) (or ZY), β_{YYY} (β_{XXX}) cancels leading to more condensed 1-D tensorial expressions:

$$\beta = \beta_{XXX}X(X^2 - 3Y^2) \quad \text{(C19)}$$

$$\text{or} \quad \beta = \beta_{YYY}Y(Y^2 - 3X^2) \quad \text{(C20)}$$

Planar molecules, such as TATB in a crystalline environment, correspond to this symmetry group.

Appendix D. Irreducible Components of Rank-3 Symmetric Tensors: 2-D and 3-D Schemes

In order to decompose the β tensor attached to a planar tensor in irreducible components, two schemes leading to different results may be followed. The purpose of this Appendix is to explore these schemes and their underlying physical implications.

First Scheme. It considers, as the initial tensor to be subsequently decomposed, the 4-D expression detailed in eq 30 following the 2-D model of ref 18. Corresponding irreducible components may be straightforwardly obtained in the Cartesian framework from the procedure mentioned in Appendix C (e.g. eq C3), leading to eqs 31 and 32 recalled hereafter in the simplified polynomial notation:

$$\beta^{2D}_{J=1} = 3/4\ [(\beta_{XXX} + \beta_{XYY})X + (\beta_{YYY} + \beta_{YXX}Y][X^2 + Y^2] \quad \text{(D1)}$$

$$\beta^{2D}_{J=3} = 1/4\ (\beta_{XXX} - 3\beta_{XYY})X(X^2 - 3Y^2) + 1/4\ (\beta_{YYY} - 3\beta_{YXX})Y(Y^2 - 3X^2) \quad \text{(D2)}$$

Adequate normalizations, complying with Pythagorean theorem and the projection closure condition, are

$$\|\beta^{2D}_{J=1}\|^2 = 3/4\ [(\beta_{XXX} + \beta_{XYY})^2 + (\beta_{YYY} + \beta_{YXX})^2] \quad \text{(D3)}$$

$$\|\beta^{2D}_{J=3}\|^2 = 1/4\ [(\beta_{XXX} - 3\beta_{XYY})^2 + (\beta_{YYY} - 3\beta_{YXX})^2] \quad \text{(D4)}$$

The superscript 2D has been introduced for reasons which will become clear in the following.

Second Scheme. It proceeds from the general decomposition detailed in Appendix C (expressions C2 and C4) where all tensor coefficients containing Z at least once are being subsequently canceled, leading to

$$4\beta^{3D}_{J=1} = 3[(\beta_{XXX} + \beta_{XYY})X + (\beta_{YXX} + \beta_{YYY})Y](X^2 + Y^2 + Z^2) \quad \text{(D5)}$$

$$\begin{aligned} 5\beta^{3D}_{J=3} = {} & (4\beta_{XYY} - \beta_{XXX})X(3Y^2 - X^2) \\ & + (4\beta_{YXX} - \beta_{YYY})Y(3X^2 - Y^2) \\ & + (\beta_{XXX} + \beta_{XYY})X(X^2 - Z^2) \\ & + (\beta_{YYY} + \beta_{YXX})Y(Y^2 - 3Z^2) \end{aligned} \quad \text{(D6)}$$

with the following normalizations:

$$\|\beta^{3D}_{J=1}\|^2 = 3/5\,[(\beta_{XXX} + \beta_{XYY})^2 + (\beta_{YXX} + \beta_{YYY})^2] \quad \text{(D7)}$$

$$\|\beta^{3D}_{J=3}\|^2 = 2/5\,(\beta^2_{XXY} + \beta^2_{YYY} + 6\beta^2_{YXX} + 6\beta^2_{XYY} - 3\beta_{YXX}\beta_{YYY} - 3\beta_{XXX}\beta_{XYY}) \quad \text{(D8)}$$

The superscript 3D points out the distinctions between expressions D5 through D8, obtained by the latter scheme, from expressions D1 through D4 with corresponding 2D superscript as from the former scheme. In spite of differences, addition of the $J = 1$ and $J = 3$ components exactly reconstructs the same 4-D β tensor as given in eq 30. The difference lies in the consideration, for the 3-D case, of out-of-plane anisotropies, as evidenced by the presence in the tensorial basis set, of Z-containing products such as Z^2X or Z^2Y, albeit associated with purely X and Y indexed tensorial coefficients, which are disregarded in the 2-D scheme. While in the 3-D approach, planar molecules are embedded in 3-D space with Z containing tensorial products sustaining out-of-plane polarizabilities, the 2-D approach constrains polarizabilities to lie exclusively in the (X,Y) molecular plane. Restricted 2-D expressions such as $\beta^{2D}_{J=3}$ given by the Cartesian expression in D2 can be equivalently expressed with respect to a spherical tensorial basis set behaving like the $Y^m_{J=3}$ spherical harmonics: it can be straightforwardly verified that only Y^3_3 and Y^{-3}_3 are then involved. On the contrary, the unrestricted 3-D expressions involve Y^3_3, Y^{-3}_3 together with Y^1_3 and Y^{-1}_3. It is worthwhile to establish and calculate the difference between β^{3D}_J and β^{2D}_J expressions so as to evidence the contribution of out-of-plane interactions in planar systems. The following tensor differences may be normalized

$$T_J = \beta^{3D}_J - \beta^{2D}_J \quad \text{(D9)}$$

with $J = 1, 3$ leading to

$$T_{J=3} = -T_{J=1} = 3/20\,[(\beta_{XXX} + \beta_{XYY})X + (\beta_{YYY} + \beta_{YXX})Y](X^2 + Y^2 - 4Z^2) \quad \text{(D10)}$$

$$\|T_{J=3}\|^2 = \|T_{J=1}\|^2 = 3/20\,[(\beta_{XXX} + \beta_{XYY})^2 + (\beta_{YYY} + \beta_{YXX})^2] = 1/5\,\|\beta^{2D}_{J=1}\|^2 \quad \text{(D11)}$$

The relative deviation α between the two schemes may be considered as the relative amount of out-of-plane contribution β namely

$$\alpha = \frac{\|T_{J=3}\|^2}{\|\beta\|^2} = \frac{\|\beta^{3D}_{J=3} - \beta^{2D}_{J=3}\|^2}{\|\beta\|^2} \quad \text{(D12)}$$

$$\alpha = 1/5\,\frac{1}{1 + (\rho^{2D})^2} \quad \text{(D13)}$$

with ρ^{2D} defined as in section II by the ratio $\|\beta^{2D}_{J=3}\|/\|\beta^{2D}_{J=1}\|$. The expressions of ρ^{3D} and ρ^{2D} are

$$\rho^{3D} = \frac{\|\beta^{3D}_{J=3}\|}{\|\beta^{3D}_{J=1}\|} = 2/3\,\frac{\beta^2_{XXX} + \beta^2_{YYY} + 6\beta^2_{XYY} + 6\beta^2_{YXX} - 3\beta_{XYY}\beta_{XXX} - 3\beta_{YXX}\beta_{YYY}}{(\beta_{XXX} + \beta_{XYY})^2 + (\beta_{YYY} + \beta_{YXX})^2} \quad \text{(D14)}$$

Table 5. Values of Parameters α and ρ^{2D} and ρ^{3D} as defined in Appendix D for Various Molecules

	u	ρ^{2D}	α	ρ^{3D}
urea	−0.52	3.09	0.019	7.11
DIODD (X = H)	−3.17	2.8	0.023	26.63
NPP	−0.134	0.93	0.11	1.42
TATB	−1	∞	0	∞

$$\rho^{2D} = \frac{\|\beta^{2D}_{J=3}\|}{\|\beta^{2D}_{J=1}\|} = 1/3\,\frac{(\beta_{XXX} - 3\beta_{XYY})^2 + (\beta_{YYY} - 3\beta_{YXX})^2}{(\beta_{XXX} + \beta_{XYY})^2 + (\beta_{YYY} + \beta_{YXX})^2} \quad \text{(D15)}$$

In the special case of C_{2v} ($mm2$) symmetry with Y as the 2-fold axis, expression D15 simplifies into eq 39, while ρ^{3D} becomes

$$\rho^{3D} = (2/3)^{1/2}\left|\frac{1 - 3u + 6u^2}{1 + u}\right| \quad \text{(D16)}$$

Values of α, ρ^{2D}, and ρ^{3D} are listed in Table 5 for three representative molecules evidencing significant differences depending on the irreducible decomposition scheme adopted.

Appendix E. Determination of Isotropically Averaged $\beta \otimes \beta$ Tensor Coefficients for Point Groups C_{2v} and D_{3h}

The scattered harmonic light intensity can be expressed as a linear combination of products of molecular hyperpolarizability coefficients expressed in a molecular reference frame. The constant coefficients in this development are obtained, in principle, from isotropic averaging of the $\beta \otimes \beta$ tensor. While such a calculation has been reported, to our knowledge, in at least two references,[55,56] serious discrepancies have been found between these: we have therefore developed our own approach to be detailed in the following and leading to results in agreement with ref 55 by Cyvin et al. while differences show up with ref 56.

We restrict our attention to molecular symmetry point groups of interest in the present experimental context, namely D_{3h} for a planar crystal violet or TATB geometry,[5] and C_{2v} for acetone or p-nitroaniline. C_{2v} may be considered as a subgroup of C_{3v} where the z 3-fold axis has been removed. We will also refer to D_3 (nonplanar propeller shape for CV where the phenyl rings are twisted out of plane) and T_d for CCl_4. Symmetry elements are represented in Figure 19, where various configurations of an hexasubstituted benzene are used to illustrate the point groups of interest. In order to maintain, for the sake of clarity, a consistent symmetry axis labeling, consistently encompassing both trigonal and polar C_{2v} groups, the y axis is nonconventionally located along the mirror intersections in the C_{2v} case, whereas the labeling follows conventions for the trigonal groups. The laboratory and molecular reference frames are depicted in Figure 20: the molecular coordinate axis $\{x,y,z\}$ are defined by Euler angles (θ,ϕ,ψ) with respect to the laboratory axis $\{X,Y,Z\}$. An intermediary spherical $\{u,v,w\}$ framework is introduced. The average $\langle F \rangle$ of a well-behaved function of the Euler angles $F(\theta,\phi,\psi)$, in our case a trigonometric polynomial

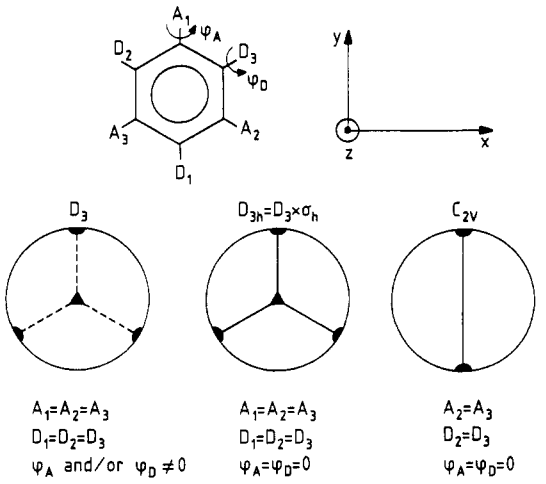

Figure 19. Various noncentrosymmetric point groups of interest in this study with a hexasubstituted aromatic ring as an illustration. The highest symmetry case D_{3h} corresponds to a planar molecule with identical substitutions respectively at the 1,3,5 and 2,4,6 sites. Removal of planarity, corresponding to nonzero torsional angles at the substituent sites, reduces D_{3h} symmetry to the D_3 point group. Similarly, a less symmetric substitution scheme reduces the D_{3h} group to the less symmetrical polar C_{2v} group.

of maximal degree 6, is obtained from

$$\langle F \rangle = \frac{1}{8\pi^2}\int F(\theta,\phi,\psi)\sin\theta\, d\phi\, d\psi \qquad \text{(E1)}$$

with $0 < \theta < \pi$, $0 < \phi < 2\pi$, and $0 < \psi < 2\pi$.

Connection between molecular and laboratory coordinates is given by the Euler matrix, namely

$$x = (\cos\psi\cos\theta\cos\phi - \sin\psi\sin\phi)\boldsymbol{X} + (\cos\psi\cos\theta\sin\phi + \sin\psi\cos\phi)\boldsymbol{Y} - (\sin\theta\cos\psi)\boldsymbol{Z} \qquad \text{(E2)}$$

$$y = (\sin\psi\cos\theta\cos\phi - \sin\phi\cos\psi)\boldsymbol{X} + (\cos\phi\cos\psi - \sin\psi\cos\theta\sin\phi)\boldsymbol{Y} + (\sin\psi\sin\theta)\boldsymbol{Z} \qquad \text{(E3)}$$

$$z = (\sin\theta\cos\phi)\boldsymbol{X} + (\sin\theta\sin\phi)\boldsymbol{Y} + (\cos\theta)\mathbf{Z} \qquad \text{(E4)}$$

Molecular symmetry considerations help reduce the number of independent tensorial coefficients which can be further reduced by Kleinman index permutation symmetry.

Relevant tensorial expressions are given below for groups D_3, C_{2v}, D_{3h}, and T_d, respectively with and without Kleinman symmetry assumptions. In the case of groups C_{2v} and D_{3h}, the nonlinearity follows a 2-D model whereby all z-containing β coefficients are assumed negligible. In the following, we use a simple homogeneous polynomial notation for tensor products with, for example, $\mathbf{xy^2}$ standing for $\mathbf{y} \otimes \mathbf{x} \otimes \mathbf{x}$.

Group D_3

Kleinman Nonvalid

$$\beta = \beta_{yyy}\mathbf{y}(\mathbf{y}^2 - 3\mathbf{x}^2) + (\beta_{yzz} + \beta_{zyz} + \beta_{zzy})\mathbf{y}(\mathbf{z}^2 - \mathbf{x}^2) + (\beta_{xyz} + \beta_{xzy} + \beta_{yxz} + \beta_{yzx} + \beta_{zxy} + \beta_{zyx})\mathbf{xyz} \qquad \text{(E5)}$$

Kleinman Valid

$$\beta = \beta_{yyy}\mathbf{y}(\mathbf{y}^2 - 3\mathbf{x}^2) + 3\beta_{yzz}\mathbf{y}(\mathbf{z}^2 - \mathbf{x}^2) + 6\beta_{xyz}\mathbf{xyz} \qquad \text{(E6)}$$

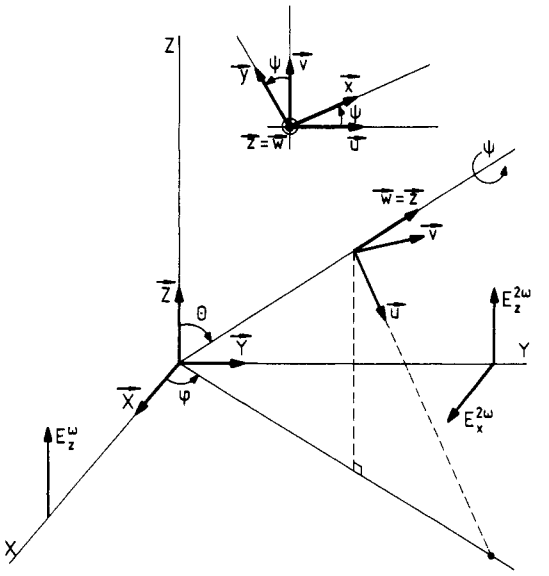

Figure 20. Different reference frames used in the averaging procedures. (X, Y, Z) is the laboratory framework with the fundamental incoming beam polarization along Z. The observation direction is along Y. The reference frame attached to individual molecules is $\{x,y,z\}$ defined by Euler angles (θ,ϕ,ψ) with respect to laboratory axis. The usual spherical framework $\{u,v,w\}$ is a convenient intermediary between the laboratory and molecular frameworks.

Group D_{3h}

$$\beta = \beta_{yyy}\mathbf{y}(\mathbf{y}^2 - 3\mathbf{x}^2) \qquad \text{(E7)}$$

In this case, symmetry constraints, namely $\beta_{yyy} = -\beta_{xyy} = -\beta_{yxy} = -\beta_{yyx}$ entail Kleinman symmetry.

Group C_{2v}

Kleinman Nonvalid

$$\beta = \beta_{yyy}\mathbf{y}^3 + (\beta_{yxx} + \beta_{xyx} + \beta_{xxy})\mathbf{yx}^2 \qquad \text{(E8)}$$

Kleinman Valid

$$\beta = \beta_{yyy}\mathbf{y}^3 + 3\beta_{yxx}\mathbf{yx}^2 \qquad \text{(E9)}$$

Group T_d

Kleinman Nonvalid

$$\beta = (\beta_{xyz} + \beta_{xzy} + \beta_{yxz} + \beta_{yzx} + \beta_{zxy} + \beta_{zyx})\mathbf{xyz} \qquad \text{(E10)}$$

Kleinman Valid

$$\beta = 6\beta_{xyz}\mathbf{xyz} \qquad \text{(E11)}$$

We detail in the following the averaging procedure for a 2-D C_{2v} molecule complying with Kleinman symmetry. The D_{3h} case will be readily obtained therefrom by introducing the additional 3-fold symmetry entailing $\beta_{yyy} = -\beta_{yxx}$.

In the experimental configuration on Figure 20, the fundamental field, linearly polarized along $\boldsymbol{Z}$, is propagating along $\boldsymbol{X}$ while the 90° off-axis observation direction is along $\boldsymbol{Y}$, with possibilities for polarized harmonic detection along $\boldsymbol{X}$ or $\boldsymbol{Z}$.

In this geometry, the macroscopic nonlinear polarizations of interest are

$$P_X^2 = \langle \mu_X^2 \rangle = \langle \beta_{XZZ} \rangle (E_Z^\omega)^2 \quad \text{(E12)}$$

$$P_Z^{2\omega} = \langle \mu_Z^2 \rangle = \langle \beta_{ZZZ} \rangle (E_Z^\omega)^2 \quad \text{(E13)}$$

Owing to the cylindrical ∞mm ($C_{\infty mm}$) macroscopic geometry of the system with respect to Z, $P_X^{2\omega} = P_Y^{2\omega}$ and $\langle \mu_X^2 \rangle = \langle \mu_Y^2 \rangle$. μ_X, μ_Y, and μ_Z are the components in the laboratory framework of the induced harmonic dipole more readily expressed in the molecular framework and derived therefrom by application of the Euler rotation matrix and subsequent isotropic averaging. We propose, rather than following this straightforward however tedious procedure, an alternative and simpler method relying on the invariance of $\langle \mu^2 \rangle$ when expressed respectively in the laboratory and molecular framework, namely

$$\langle \mu \rangle^2 = 2\langle \mu_X^2 \rangle + \langle \mu_Z^2 \rangle = \langle \mu_x^2 \rangle + \langle \mu_y^2 \rangle \quad \text{(E14)}$$

In this expression, we assume a negligible out-of-plane nonlinearity ($\mu_Z = 0$) and a cylindrical macroscopic symmetry as previously stated.

While the expression of μ_Z^2 in terms of the Euler angles is relatively simple and compatible with a tractable averaging procedure as a consequence of the simplifying Z-cylindrical $C_{\infty v}$ symmetry, μ_X^2 ($= \mu_Y^2$) takes a markedly more complicated form. On the contrary, $\langle \mu_x^2 \rangle + \langle \mu_y^2 \rangle$ takes a simpler expression which can be straightforwardly averaged in contrast with μ_X^2. Finally, $\langle \mu_X^2 \rangle$ may be obtained therefrom, by virtue of expression E14, by following

$$\langle \mu_X^2 \rangle = \langle \mu_Y^2 \rangle = 1/2\,[\langle \mu_x^2 \rangle + \langle \mu_y^2 \rangle - \langle \mu_Z^2 \rangle] \quad \text{(E15)}$$

In the case of C_{2v} symmetry (encompassing the D_{3h} case), the relevant squared dipole components to be averaged are given by

$$\mu_Z^2 = \sin^6\theta \sin^2\psi\,[9\beta_{yxx}^2 \cos^4\psi + \beta_{yyy}^2 \sin^4\psi + 6\beta_{yxx}\beta_{yyy} \sin^2\psi \cos^2\psi] \quad \text{(E16)}$$

$$\mu_x^2 + \mu_y^2 = \sin^4\theta\,[\beta_{yxx}^2 \cos^2\psi\,(1 + 3\sin^2\psi) + \beta_{yyy}^2 \sin^4\psi + 2\beta_{yyy}\beta_{yxx} \sin^2 2\psi] \quad \text{(E17)}$$

These expressions, and the following, are normalized with respect to $(E_Z^\omega)^2$ so as to simplify notations.

Straightforward angular averaging of the various trigonometric polynomial expressions above leads to

$$\langle \mu_Z^2 \rangle = 9/35\,\beta_{yxx}^2 + 1/7\,\beta_{yyy}^2 + 6/35\,\beta_{yxx}\beta_{yyy} \quad \text{(E18)}$$

$$\langle \mu_x^2 \rangle + \langle \mu_y^2 \rangle = 7/15\,\beta_{yxx}^2 + 1/5\,\beta_{yyy}^2 + 2/15\,\beta_{yyy}\beta_{yxx} \quad \text{(E19)}$$

$\langle \mu_X^2 \rangle$ is then readily obtained by application of eq E15:

$$\langle \mu_X^2 \rangle = \langle \mu_Y^2 \rangle = 1/35\,\beta_{yyy}^2 + 11/105\,\beta_{yxx}^2 - 2/105\,\beta_{yyy}\beta_{yxx} \quad \text{(E20)}$$

These expressions can be further reduced, by incorporation of D_{3h} symmetry constraints, to

$$\langle \mu_Z^2 \rangle = 8/35\,\beta_{yyy}^2 \quad \text{(E21)}$$

$$\langle \mu_X^2 \rangle = \langle \mu_Y^2 \rangle = 16/105\,\beta_{yyy}^2 \quad \text{(E22)}$$

As shown in section V and Table 4, these expressions can also be derived by automatic application of the procedure detailed by Cyvin et al.[55] These common results, established by two independant procedures, disagree with those obtained by application of the expressions in the Appendix B of ref 56, which, we believe, are erroneous. Expressions for groups T_d and D_3 may also be found in Table 4.

References

(1) Zyss, J. *Nonlinear Opt.* **1991**, *1*, 3.
(2) Zyss, J. *J. Chem. Phys.* **1993**, *98*, 6583.
(3) Zyss, J. In *Nonlinear Optics: Fundamentals, Materials and Devices*; Miyata, S., Ed.; North Holland: Amsterdam, 1992; pp 33–48.
(4) Zyss, J.; Ledoux, I.; Nicoud, J.-F. In *Molecular Nonlinear Optics: Materials, Physics and Devices*; Zyss, J., Ed.; Academic Press: Boston, 1993.
(5) Ledoux, I.; Zyss, J.; Siegel, J.; Brienne, J.; Lehn, J.-M. *Chem. Phys. Lett.* **1990**, *172*, 440.
(6) Zyss, J.; Dhenaut, C.; ChauVan, T.; Ledoux, I. *Chem. Phys. Lett.* **1993**, *206*, 409.
(7) Brédas, J.-L.; Meyers, F.; Pierce, B.; Zyss, J. *J. Am. Chem. Soc.* **1992**, *114*, 4928.
(8) Joffre, M.; Yaron, D.; Silbey, R. J.; Zyss, J. *J. Chem. Phys.* **1992**, *97*, 5607. Pierce, B. M.; Zyss, J.; Joffre, M. *SPIE Proc.* **1993**.
(9) Zyss, J.; Chemla, D. S.; Nicoud, J.-F. *J. Chem. Phys.* **1981**, *74*, 4800.
(10) Barzoukas, M.; Blanchard-Desce, M.; Josse, D.; Lehn, J.-M.; Zyss, J. *Chem. Phys.* **1989**, *33*, 323.
(11) Wigner, E. P. *Group Theory*; Academic Press: New York, 1959.
(12) Butcher, P. N. Nonlinear Optical Phenomena. Ohio State University, 1965.
(13) Jerphagnon, J. *Phys. Rev. B* **1970**, *2*, 1091.
(14) Chemla, D. S.; Oudar, J.-L.; Jerphagnon, J. *Phys. Rev. B* **1975**, *12*, 4534.
(15) Jerphagnon, J.; Chemla, D. S.; Bonneville, R. *Adv. Phys.* **1978**, *27*, 609.
(16) Cady, H. H.; Larson, A. C. *Acta Crystallogr.* **1965**, *18*, 485.
(17) Schwartz, L. *Les Tenseurs*; Hermann: Paris, 1981.
(18) Oudar, J.-L.; Zyss, J. *Phys. Rev. A* **1982**, *26*, 2016.
(19) Zyss, J.; Oudar, J. L. *Phys. Rev. A* **1982**, *26*, 2028.
(20) Nalwa, H. S.; Nakajima, K.; Watanabe, T.; Nakamura, K.; Yamada, A.; Miyata, S. *Jpn. J. Appl. Phys.* **1991**, *30*, 983.
(21) Zyss, J.; Nicoud, J.-F.; Coquilllay, M. *J. Chem. Phys.* **1984**, *81*, 4160.
(22) Vidakovic, P.; Coquillay, M.; Salin, F. *J. Opt. Soc. Am. B* **1987**, *4*, 998.
(23) Barzoukas, M.; Josse, D.; Frémaux, P.; Zyss, J.; Nicoud, J.-F.; Morley, J. O. *J. Opt. Soc. Am. B* **1987**, *4*, 967.
(24) Zyss, J.; Berthier, G. *J. Chem. Phys.* **1982**, *77*, 3635.
(25) Oudar, J.-L.; Hierle, R. *J. Appl. Phys.* **1977**, *48*, 2669.
(26) Boulanger, B.; Marnier, G. *J. Phys.: Condens. Mater.* **1991**, *3*, 8327.
(27) Brédas, J.-L.; Déhu, C.; Meyers, F.; Persoons, A.; Zyss, J. *Nonlinear Opt.* **1993**, in press.
(28) Verbiest, T.; Clays, K.; Persoons, A.; Meyers, F.; Brédas, J.-L. *Opt. Lett.* **1993**, *18*, 525.
(29) Zyss, J.; Chauvan, T.; Dhenaut, C.; Ledoux, I. *Chem. Phys.* **1993**, *177*, 281.
(30) Terhune, R. W.; Maker, P. D.; Savage, C. M. *Phys. Rev. Lett.* **1965**, *14*, 681.
(31) Maker, P. D. *Phys. Rev. A*, **1970**, *1*, 923.
(32) Clays, K.; Perssons, A. *Phys. Rev. Lett.* **1991**, *66*, 2980; *Rev. Sci. Instrum.* **1992**, *63*, 3285.
(33) Gund, P. *J. Chem. Educ.* **1972**, *49*, 101.
(34) Grajcar, L.; Berthier, G.; Faure, J.; Fleury, J.-P. *Theor. Chim. Acta* **1987**, *71*, 299.
(35) Wolff, J. J.; Nelsen, S. F.; Petillo, P. A.; Powell, R. D. *Chem. Ber.* **1991**, *124*, 1719. Wolff, J. J.; Nelsen, S. F.; Powell, R. D. *J. Org. Chem.* **1991**, *56*, 5908.
(36) Lazzeretti, P.; Tossell, J. A. *J. Mol. Struct. (Theochem)* **1991**, *236*, 403.
(37) Heilbronner, E.; Bock, H. *Das HMO-Modell und seine Anwendung*; Verlag Chemie: Weinheim; 1970; Vol. II, p 365.
(38) Zyss, J. *J. Chem. Phys.* **1979**, *70*, 3333; **1979**, *70*, 3341; **1979**, *70*, 909.
(39) Marder, S. R.; Beratan, D. N.; Cheng, L.-T. *Science* **1991**, *252*, 103.
(40) Oudar, J.-L. *J. Chem. Phys.* **1977**, *67*, 446.
(41) Buckingham, A. D.; Disch, R. L. *Proc. R. Soc.* **1963**, *A273*, 275.
(42) French, M. J. *Hyper Rayleigh and Hyper Raman Spectroscopy, in Chemical Applications of Raman Spectroscopy*; Academic Press: New York, 1981.
(43) Zyss, J.; Pécaud, J.; Lévy, J.-P.; Masse, R. *Acta Crystallogr. B* **1993**, *49*.
(44) Loucif-Saïbi, R.; Delaire, J.; Bonazzola, L.; Doisneau, G.; Balavoine, G.; Fillebeen-Khan, T.; Ledoux, I.; Puccetti, G. *Chem. Phys.* **1992**, *167*, 369.
(45) Andreazza, P.; Josse, D.; Lefaucheux, F.; Robert, M. C.; Zyss, J. *Phys. Rev. B* **1992**, *45*, 7640.

(46) Davis, P. J.; Hall, S. R.; Jones, R. J.; Kolinsky, P. A.; Weinel, A. J.; Hursthouse, M. B.; Karaulov, S. A. In *Organic Materials for Nonlinear Optics*; Hann, R. A., Bloor, D., Royal Society of Chemistry: London, 1989; p 163.
(47) Stora, C. *C. R. Acad. Sci. Ser. 2* **1958**, *246*, 1693.
(48) Lueck, H. B.; McHale, J. L.; Edwards, W. D. *J. Am. Chem. Soc.* **1992**, *114*, 2342.
(49) Lewis, G. N.; Magel, T. T.; Lipkin, D. J. *J. Am. Chem. Soc.* **1942**, *64*, 1774.
(50) Dekkers, H. P.; Kielman-van Luyt, E. C. *Mol. Phys.* **1976**, *31*, 1001.
(51) Belsen, P. D.; Daul, C.; von Zelewsky, A. *Chem. Phys. Lett.* **1981**, *79*, 596.
(52) Green, M. L. H.; Marder, S. R.; Thompson, M. E.; Bandy, J. A.; Bloor, D.; Kolinsky, P. V.; Jones, R. J. *Nature* **1987**, *330*, 360.
(53) Laidlaw, W. M.; Denning, R. G.; Verbiest, T.; Chauchard, E.; Persoons, A. *Nature* **1993**, *363*, 58.
(54) Kielich, S. *Bull. Acad. Pol. Sci.* **1964**, *12*, 53.
(55) Cyvin, S. G.; Rauch, J. E.; Decius, J. C. *J. Chem. Phys.* **1965**, *43*, 4083.
(56) Bersohn, R.; Pao, Y. H.; Frisch, H. L. *J. Chem. Phys.* **1966**, *45*, 3184.
(57) Meyers, F.; Brédas, J.-L.; Zyss, J. *J. Am. Chem. Soc.* **1992**, *114*, 2914.
(58) Chen, C. T.; Wu, B.; Jiang, A.; You, G. *Sci. Sinica* **1985**, *28*, 235.
(59) Willand, C. S.; Albrecht, A. C. *Opt. Commun.* **1985**, *57*, 146.
(60) Xu, D.; Jiang, M.; Tan, Z. *Acta Chim. Sinica* **1983**, *2*, 230.
(61) Eimerl, D.; Velsko, S.; Davis, L.; Wang, F.; Loiacono, G.; Kennedy, G. *IEEE J. Quant. Electron.* **1989**, *QE25*, 179.
(62) Singer, K. D.; Kuzyk, M.; Sohn, J. *J. Opt. Soc. Am. B* **1987**, *4*, 968.
(63) Charra, F.; Devaux, F.; Nunzi, J. M.; Raimond, P. *Phys. Rev. Lett.* **1992**, *68*, 2440.
(64) Nunzi, J. M.; Charra, F.; Fiorini, C.; Zyss, J. *Chem. Phys. Lett.*, submitted for publication.
(65) Osterberg, U.; Margulis, W. *Opt. Lett.* **1986**, *11*, 516.
(66) Baranova, N. B.; Zel'dovich, B. Ya. *JETP Lett.* **1987**, *45*, 716.
(67) Zyss, J.; Nunzi, J. M.; Charra, F.; Fiorini, C. To be published.
(68) Yariv, A. *Quantum Electronics*; Wiley: New York, 1989.